



Adsorption of lead ion by a polyether sulphone-type chelating membrane bearing aminophosphonic acid functional groups

Laizhou Song^{a,*}, Min Ji^a, Baoyou Shi^{b,*}, Cai Wang^a, Xiuli Wang^a, Pei Liu^a

^aCollege of Environmental and Chemical Engineering, Yanshan University, Qinhuangdao, 066004, China, Tel. +86 335 8061569; Fax: +86 3358061569; email: songlz@ysu.edu.cn (L. Song), Tel. +86 3358387741; Fax: +86 3358061569; email: 18332552913@163.com (M. Ji), Tel. +86 3358061422; Fax: +86 3358061569; email: caiw1014@163.com (C. Wang), Tel. +86 3358061569; Fax: +86 3358061569; email: xtwang7904@ysu.edu.cn (X. Wang), Tel. +86 3358061422; Fax: +86 3358061569; email: liupeil18330367815@163.com (P. Liu)

^bResearch Center for Eco-Environmental Sciences, Chinese Academy of Sciences, Beijing, 100085, China, Tel. +86 10 62924821; Fax: +86 10 62924821; email: byshi@rcees.ac.cn

Received 18 July 2018; Accepted 12 December 2018

ABSTRACT

A polyether sulphone (PES)-type chelating membrane containing aminophosphonic acid groups was fabricated for the purpose of Pb(II) removal from the aqueous solution. Effects of pH, initial Pb(II) concentration, temperature, contact time, thickness of membrane stack, flow rate, three coexisting cations (Cd(II), Ni(II) and Cu(II)), and three complexing reagents (citric acid, nitrilotriacetic acid and ethylenediaminetetraacetic acid) on the Pb(II) adsorption by the membrane were evaluated. The adsorption kinetics, adsorption isotherms and breakthrough curves with the presence of the six coexisting substances were studied. The adsorption–diffusion partial differential equations for Pb(II) adsorption were analyzed and verified by energy dispersive X-ray spectroscopy and X-ray photoelectron spectroscopy. In addition, the reused performance of the membrane was evaluated. The presence of coexisting substances reduces the Pb(II) uptake, Cu(II) and ethylenediaminetetraacetic acid show a more remarkable interference than other cations and complexing reagents. The Langmuir and pseudo-second-order models are competent for the description in adsorption isotherms and adsorption kinetics; the breakthrough process can be described by the bed depth service time model. The Pb(II) adsorption is a spontaneous and exothermic process. When Pb(II) permeates through the membrane stack, the decrease of this metal uptake along the axial depth direction is validated.

Keywords: Polyether sulphone-type chelating membrane; Heavy metal adsorption; Coexisting substance; Breakthrough curve; Adsorption–diffusion partial differential equation.

1. Introduction

Heavy metal pollutants such as Pb(II), Ni(II), Cd(II), Hg(II), Cr(VI) and Cu(II) endow the characteristics of refractory biodegradation, tending to accumulation in the food chain, convenient transportation among the biological chain as well as variable state, and thus resulting in hazardous effects on ecological environment and human being health [1]. Wastewater containing Pb(II) derived from battery, petroleum, gasoline, paint, glassware and electroplating industries

has received a tremendous attention due to its considerable biotoxicity [2]. Pb(II) pollutant can cause damage to liver, kidney, brain, central nervous and reproductive systems as well as basic cellular processes [3]. Also, this pollutant may result in severe symptoms of weakness, abdominal pain and even death. Thus, the Pb(II)-containing effluent should be tremendously treated before discharge [4]. It is unambiguously urgent to exploit sufficient, robust and cost-effective techniques for the removal of this metal ion from aqueous solution, to guarantee the drained effluent being harmless.

* Corresponding authors.

Up to present, techniques of chemical precipitation and coagulation [5,6], ion exchange [7], biological treatment [8], membrane separation [9], adsorption [10,11] have been explored to remove Pb(II) from aqueous solutions. Among these approaches, the adsorption process has been extensively employed for the disposal of metal pollutants, on account of the efficient and economical features and the competent ability for recycling of metal ions from the dilute solution. Currently, in terms of merits of easy fabrication, effective cost, nonexistence of phase change, and high disposal efficiency, the membrane separation process is drawing an increasing concern for the removal of heavy metals [12–14]. From an engineering perspective, electrodialysis, reverse osmosis, nanofiltration and colloid- or polymer-enhanced ultrafiltration membrane techniques [9,15–17] have been already employed to remove metal pollutants. But the defects including high operating cost as well as superfluous pretreatment or post-treatment retard their wide applications. Compared with membrane processes above-mentioned, low pressure-driven microfiltration and ultrafiltration membrane techniques can be considered as the substitute because of the high permeation flux and nonstrict pretreatment. However, the conventional modules of these two membranes cannot capture the dissolved metal pollutants. With this regard, alternatives of these two membranes with the function of metal capture deserve to be developed. As well known, some powder-type adsorbents assembled by pentaethylenhexamine, nitrilotriacetic acid (NTA), ethylenediaminetetraacetic acid (EDTA), diethylenetriaminepentaacetic acid (DTPA), ethylenediamine tetramethylene phosphonic acid (EDTMPA), and hyperbranched polyamidoamine (HPAMAM) chelating groups [18–24] exhibit a significant performance in removal of metal ions. But, the inconveniently recycling defect constrains engineering applications of these adsorbents. Being similar to the aforementioned adsorbents with the equivalent adsorption efficiency in trapping metal pollutants, alternatives of microfiltration and ultrafiltration membranes bearing some aforesaid chelating groups (such as EDTMPA and DTPA) are manifested to be competent for the removal of heavy metals [21–24].

The polyether sulphone (PES) separation membrane has been widely used in water treatment field because of its excellent chemical stability, anti-fouling performance and prominent mechanical property [25]. To unravel the conundrum of conventional PES microfiltration and ultrafiltration membranes incapable of capturing heavy metals via an adsorption process, the incorporation of ion-exchange and/or chelating groups into PES polymer matrix has been attempted [26]. The grafting of amino functional groups into PES molecular chain can capture heavy metal ions from wastewater [27,28]. However, the removal efficiencies in some metal pollutants (such as Pb(II), Ni(II) and Cd(II)) are undesirable. Although the physical blending of DTPA, EDTMPA, HPAMAM and other chelating groups with the form of colloid microparticles into the membrane matrix will be applicable for the removal of metal ions [29,30], defects involving the heterogeneity distribution of blended microparticles, and the decrease in filtration flux and surface pore size cannot be ignored [31]. The nitrogen and oxygen atoms of amino phosphonic acid and amino carboxylic acid possess strong electronegativity, exhibiting an excellent affinity to heavy metal ions [29,30]. Hence, amino phosphonic acid or amino carboxylic

acid group incorporated into PES molecular chain by a chemical grafting process will be expected to sufficiently capture heavy metal ions from the aqueous solution. With regard to this consideration, the PES membrane matrix modified with amino phosphonic acid functional group via a chemical grafting reaction can be recommended: the PES molecular chain is first aminated to introduce the amine group, and then the incorporated amine group is phosphorylated; so the anchored aminophosphonic acid functional group will be more competent than the amine group for removal of heavy metal pollutants. To our knowledge so far, insufficient effort has focused on the modification of PES membrane via the above-mentioned route to boost the capture of metal pollutants.

In this study, we aim to offer an effective method for the removal of Pb(II) from electroplating effluent via the membrane adsorption process. Thus, a PES-type chelating membrane bearing aminophosphonic acid functional group was fabricated and employed to remove Pb(II) from aqueous solutions. The morphology, chemical components and groups of the fabricated chelating membrane were characterized using field emission scanning electron microscopy (FE-SEM), energy dispersive X-ray spectroscopy (EDS) and X-ray photoelectron spectroscopy (XPS). The batch and continuous adsorption tests for Pb(II) uptake by the membrane were carried out. Effects of pH, temperature, contact time, initial Pb(II) concentration, membrane thickness and flow rate on the uptake of this metal were evaluated. Also, effects of coexisting Cu(II), Ni(II) and Cd(II) three cations, as well as citric acid (CA), NTA and EDTA three complexing reagents were assessed. The adsorption kinetics and adsorption isotherms of Pb(II) adsorption were investigated at the presence of the coexisting cations and complexing reagents. The breakthrough curves were determined by continuous filtration tests, and obtained data were analyzed by the bed depth service time (BDST) model. The adsorption–diffusion partial differential equations (PDEs) related to Pb(II) throughout the membrane stack were analyzed and validated by EDS and XPS measurements. In addition, the reused property of this membrane was evaluated.

2. Experimental methods

2.1. Materials

PES (Ultrason E6020) powders with a molecular weight ca. 58,000 were provided by BASF (Ludwigshafen, Germany). The reagents of trichloromethane, N,N-dimethylacetamide (DMAc), diethylenetriamine (DETA), triethylamine, paraformaldehyde, anhydrous phosphorous acid, $\text{Pb}(\text{NO}_3)_2$, $\text{Cd}(\text{NO}_3)_2 \cdot 4\text{H}_2\text{O}$, $\text{Ni}(\text{NO}_3)_2 \cdot 6\text{H}_2\text{O}$, $\text{Fe}(\text{NO}_3)_3 \cdot 9\text{H}_2\text{O}$, CA, NTA, EDTA, absolute ethanol, sodium acetate, glacial acetic acid, hydrochloric acid (36.5 wt%) and sodium carbonate were purchased from Jingchun Scientific Co., Ltd. (Shanghai, China); other reagents including chloroacetyl chloride and anhydrous aluminum trichloride were purchased from Kemiou Chemical Reagent Co., Ltd. (Tianjin, China). All the reagents were of analytical grade and used as received. The stock solution of Pb(II) (100 mmol L^{-1}) and those of coexisting cations (100 mmol L^{-1}) and complexing reagents (100 mmol L^{-1}) were prepared by dissolving weighed amounts of $\text{Pb}(\text{NO}_3)_2$ and the corresponding cation-containing salts and complexing

reagents in deionized water. The Pb(II) working solutions were prepared by diluting the stock solution to appropriate volumes.

2.2. Preparation of PES-type chelating membrane

First, PES powders were chloroacetylated and this process was carried out based on our previous work [27]. For the chloroacetylation process, the additions of PES polymer, chloroform, anhydrous aluminum trichloride and chloroacetyl chloride were 6 g, 90 mL, 4 g and 4 mL, respectively; the reaction temperature and time were 313 K and 6 h. After the chloroacetylation pretreatment, the PES powders were dissolved into 30 mL DMAc, then 4 mL DETA was added to the solution. The temperature of this solution was kept at 343 K, and the bonding interaction between chloroacetylated PES and DETA occurred 4 h at this temperature. After that, 4 mL CH₃COOH (5 wt%) solution was added to the solution and followed by stirring another 2 h to obtain the casting solution. The aminated PES membrane (DETA-PES) was fabricated via a phase transfer process with deionized water as the coagulation bath and the clean glass plates as casting supports.

The obtained DETA-PES membrane was pulverized and followed by soaking adequately using 50 mL anhydrous methanol, then 24 mL triethylamine, 12 g paraformaldehyde were added to the soakage solution, and the solution was stirred 4 h at 333 K. Then, 4 mL concentrated hydrochloric acid and 24 g phosphorous acid were added to the above-mentioned soakage solution. The temperature of this solution was controlled at 368 K using water bath, and the phosphorylation procedure of DETA-PES membrane debris was carried out 6 h. Afterward, the membrane debris was collected, cleaned with deionized water and followed by drying at 333 K.

The preparation process of PES-type chelating membrane was shown as follows. First, 4.5 g phosphorylated DETA-PES membrane debris was stirred dissolved in 25 mL DMAc at 353 K, then 4 mL CH₃COOH (5 wt%) aqueous solution was added to the solution and it was stirred for 4 h. After that, the PES-type chelating membrane was fabricated using the similar phase transfer method mentioned earlier. Lastly, the fabricated membrane was soaked in 2 wt% sodium carbonate aqueous solution to form the porous structure of this membrane. For the purpose of comparison in Pb(II) uptake, except for DETA-PES membrane, the pristine PES membrane was also prepared. The preparation process of PES-type chelating membrane and the uptake of Pb(II) is depicted by Fig. 1.

2.3. Membrane characterization

The surface and cross-sectional morphologies of PES-type chelating membrane were monitored by a SUPRA55 FE-SEM (Zeiss, Germany). The functional groups of the membrane were detected by a E55+FRA106 Fourier transform infrared spectroscopy (FTIR, Bruker, Germany). Before and after adsorption of Pb(II), an EDS attached to the previously mentioned microscope was employed to determine chemical components of the membrane. Also, an X-ray photoelectron spectrometer (XPS) (ESCALAB 250, Thermo Fisher, UK) with Al K α as the radiation source was used to characterize the elements of the membrane, where the C 1s peak from

graphitic carbon at 284.6 eV was employed to calibrate the binding energy. The existing form of Pb(II) was analyzed by the HySS 2009 code. Additionally, filtration flux, mean pore size and point of zero charge (pH_{pzc}) of this chelating membrane were measured by the water permeability method and a batch equilibration method [27,31,32], respectively.

2.4. Adsorption experiments

2.4.1. Static adsorption test

The series of static adsorption tests were carried out in 200 mL Pb(II)-containing solutions, each test was performed in triplicate and the average adsorption capacity of Pb(II) was adopted. The effect of pH on the adsorption of Pb(II) was evaluated at 298 K by keeping the contact time as 1 h and chelating membrane addition at 0.1 g; pH value of the solution was adjusted to a range of 1–7 using a buffer solution consisting of 0.2 mol L⁻¹ acetic acid and 0.2 mol L⁻¹ sodium acetate. The determined optimum pH value was employed for all other adsorption processes. For the single Pb(II) system, the influences of contact time and temperature (288, 298 and 308 K) were evaluated in 200 mL solution; the initial concentration of Pb(II) and addition of chelating membrane were 1.0 mmol L⁻¹ and 0.1 g, respectively. At the different time interval (i.e., 5, 10, 30 and 60 min), 1 mL aliquot was taken from the solution and then Pb(II) concentration was determined by an atomic absorption spectrophotometer (AA6800, Shimadzu, Japan). The adsorbed amount of Pb(II) at time t (q_t , mmol g⁻¹) by the chelating membrane was obtained as that:

$$q_t = [(c_0 - c_t) \times V] / M \quad (1)$$

where c_0 and c_t (mmol L⁻¹) are the Pb(II) concentration at initial time and time t , respectively, M (g) the dry weight of the chelating membrane, and V (L) is the volume of the aqueous solution. The derived data at 298 K was employed for the analysis of adsorption kinetics. At the condition of adsorption equilibrium, the isotherm adsorption test were performed at different initial Pb(II) concentrations (0.2–1.2 mmol L⁻¹) with 0.5 g L⁻¹ addition of the membrane debris; based on this test, the effect of initial Pb(II) concentration on the uptake of this metal was also assessed.

The studies of adsorption kinetics and isotherm adsorption for other six systems with regard to the existence of Cu(II), Ni(II), Cd(II), CA, NTA and EDTA were conducted by the same methods as those of the single Pb(II) system at 298 K. All concentrations of coexisting substances and Pb(II) were 1.0 mmol L⁻¹.

2.4.2. Continuous filtration test

The continuous experiments were performed at 298 K using a single-pass membrane module with Pb(II)-containing effluent circulating back to influent, where the membranes with a thickness of 180 μ m and a diameter of 50 mm were enclosed layer by layer. The setup of membrane stack and the detailed filtration process can be referred to our previous report [33]. The flow rate was controlled by adjusting the pressure taps in inlet and outlet, and the temperature of the influent was maintained using a heat-exchanger. During

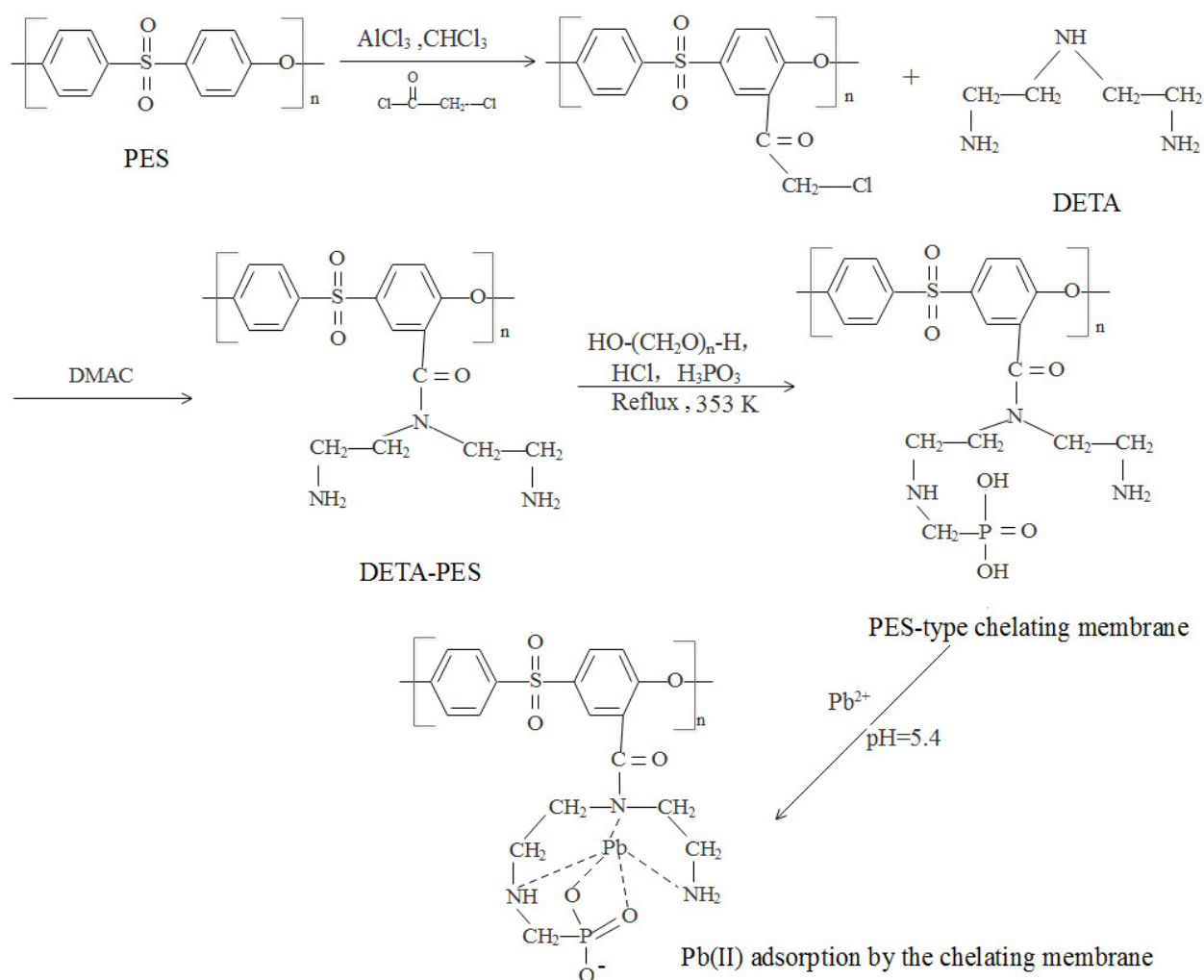


Fig. 1. Schematic diagram of preparation for the PES-type chelating membrane and the uptake of Pb(II).

the adsorption filtration, influent containing 1 mmol L⁻¹ Pb(II) with pH value of 5.4 was pumped through the membrane stack. Periodically, 1 mL of effluent was withdrawn to determine the residual Pb(II) concentration. Thus, influences of flow rate (0.28, 0.46 and 0.57 cm min⁻¹) and thickness of membrane stack (0.18, 0.36 and 0.72 mm) on the Pb(II) uptake were assessed.

The breakthrough curves for single Pb(II) and other six coexisting systems were tested at 298 K using the aforementioned single-pass membrane setup; herein, not being perfectly similar to above-described process, the effluent was not circulated back to influent. Keeping the flow rate at 0.46 cm min⁻¹, the solutions were pumped through above-mentioned three membrane stacks with different thicknesses mentioned earlier, and the effluent was collected from the outlet to measure the concentration of Pb(II) at different intervals (0, 10, 30 and 60 min). During the test, the difference in pressure at inlet and outlet (namely, transmembrane pressure [TMP]) was recorded. The obtained breakthrough curves were analyzed by the BDST model. The linear relationship between membrane stack thickness (Z) and the breakthrough time (t_b) at the point with the concentration ratio between effluent and influent as 0.05 of this model is shown as follows [34]:

$$t_b = \frac{N_0}{c_0 v} Z - \frac{1}{K_a c_0} \ln \left(\frac{c_0}{c_i} - 1 \right) \quad (2)$$

where N_0 is the saturated adsorption capacity of the membrane stack (mmol L⁻¹), c_0 (mmol L⁻¹) is the initial Pb(II) concentration in influent, c_i (mmol L⁻¹) is the concentration of this metal at time t , and v is the linear velocity (cm min⁻¹). K_a represents the rate constant (L min⁻¹ mmol⁻¹).

2.5. Analysis of adsorption–diffusion PDEs

2.5.1. Model and assumption

The filtration models for describing Pb(II) through the chelating membrane are depicted by Fig. 2, and the 2D model was employed to analyze PDEs. To describe the distribution pattern of Pb(II) passing through the chelating membrane along the sectional thickness direction, the following assumptions [35–37] were made: (1) the unsteady state convection–diffusion equation coupled by the Langmuir adsorption isotherm can adequately describe behavior of the system; (2) Pb(II) is considerably adsorbed by the deionized

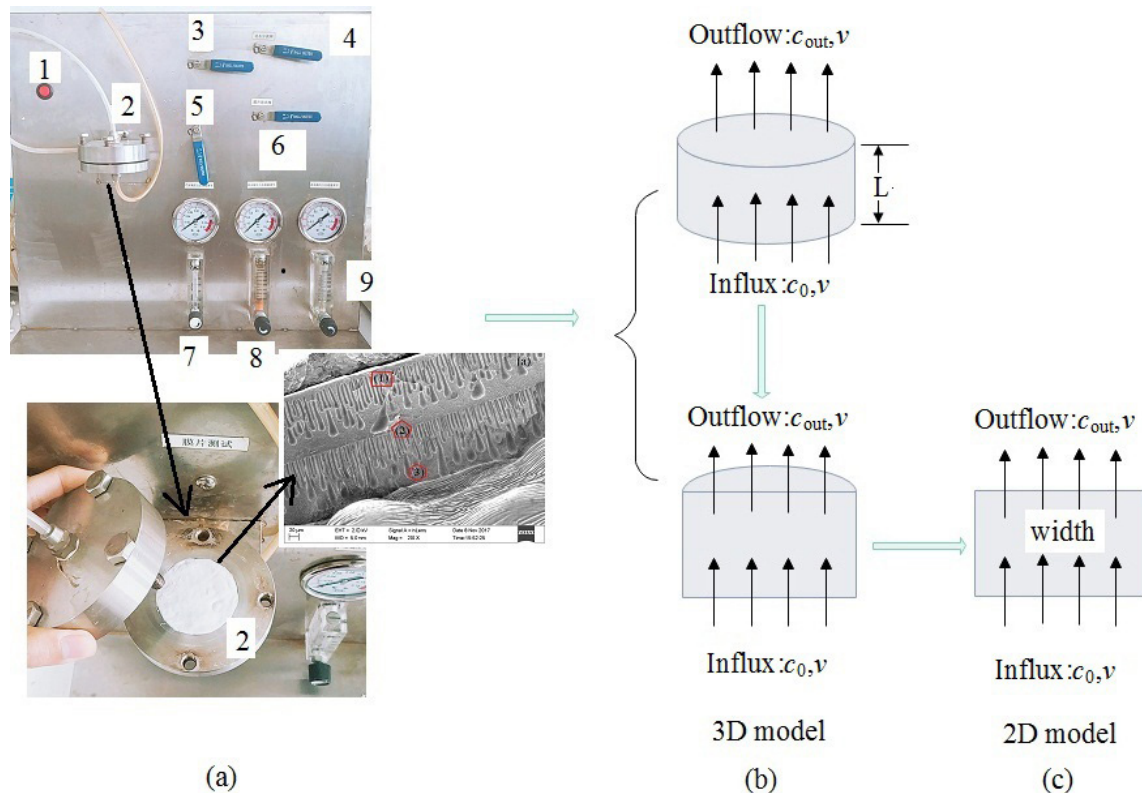


Fig. 2. Diagram illustration of Pb(II) throughout membrane stack: (a) the membrane filtration setup with a three-layered membrane stack (1—power button, 2—membrane test cell, 3—outlet valve, 4—side valve, 5—inlet valve, 6—crossflow valve, 7—outflow pressure gauge and flowmeter, 8—crossflow pressure gauge and flowmeter, 9—inlet pressure gauge and flowmeter); (b) 3D model; (c) 2D model.

aminophosphonic acid groups of chelating membrane; (3) the chelating groups on the membrane surface have no influence on adsorption and transfer of Pb(II) through the membrane; (4) Pb(II) transfers through the membrane is only in thickness direction and no any considerable dispersion, that is, the radial diffusion, radial convection and surface diffusion are negligible; (5) the internal porosity of the membrane and the transmission velocity of Pb(II) through the membrane remain constant during the filtration process, and the diffusivity of this metal is independent from other coexisting substances; (6) the accumulation of Pb(II) via the adsorption process does not change the bulk porosity of the membrane.

2.5.2. Adsorption–diffusion equation

The temporal and spatial variations in Pb(II) uptake along the membrane thickness direction can be described by the following basic mass balance equation (Eq. (3)) [38,39]:

$$\varepsilon \times \frac{\partial c}{\partial t} + (1 - \varepsilon) \times \frac{\partial q}{\partial t} = \varepsilon \times D \times \frac{\partial^2 c}{\partial z^2} - \varepsilon \times u \times \frac{\partial c}{\partial z} \quad (3)$$

In the left-hand side of Eq. (3), the first term hints the change in equilibrium concentration of Pb(II) in the solution, and the second term indicates the equilibrium concentration of this metals in the membrane (i.e., the amount uptake of this metal by the membrane). While two terms in the right-hand

side represent the rate of Pb(II) transfer across the membrane due to diffusion and convection. Where, ε is membrane bulk porosity, t is the time, c is the equilibrium concentration of Pb(II) in the solution adjacent to membrane, q is the equilibrium concentration of Pb(II) in membrane (the amount of Pb(II) captured by the membrane), D is the diffusivity of Pb(II), and u is the superficial velocity of the feed. z indicates the axial coordinate, also indicating the thickness direction along the membrane. The initial and boundary conditions corresponding to Eq. (3) are described as follows [38,39]:

$$c = 0, \text{ at } z \geq 0, t = 0 \quad (4)$$

$$q = 0, \text{ at } z \geq 0, t = 0 \quad (5)$$

$$\varepsilon \times u \times c - \varepsilon \times D \times \frac{\partial c}{\partial z} = \varepsilon \times u \times c_0, \text{ at } z = 0, t > 0 \quad (6)$$

$$\frac{\partial c}{\partial z} = 0, \text{ at } z = L, t > 0 \quad (7)$$

where L is the thickness of the membrane stack, and c_0 is the initial concentration of Pb(II) in the feed. $z = 0$, and $z = L$ present the positions of the top end and the lowest end of

membrane stack, respectively. For the Pb(II) distribution between membrane and solution, the adsorption/desorption equilibrium was employed to describe the Langmuir isotherm. This isotherm involves a second-order kinetic reversible process between adsorption and desorption, which is shown as follows [35,40]:

$$\frac{\partial q}{\partial t} = k_{\text{ads}} \times c \times (q^* - q) - k_{\text{des}} \times q \quad (8)$$

herein q^* is the maximum possible concentration of Pb(II) in the membrane; k_{ads} and k_{des} are the adsorption and desorption rate constants, respectively. The set of equations mentioned earlier (Eqs. (3)–(8)) describing the behavior of Pb(II) through membrane stack were analyzed by the chemical engineering code in Comsol Multiphysics 5.2 software. The above-mentioned parameters were valued as follows: 0.36 mm for L , 1 mmol L⁻¹ for c_0 , 0.53 L mol⁻¹ s⁻¹ for k_{ads} , 5.24×10^{-5} s⁻¹ for k_{des} , 2.0 mmol L⁻¹ for q^* , 9.45×10^{-8} m² s⁻¹ for D , 7.72×10^{-5} m s⁻¹ for u , and 0.5 for ϵ .

2.6. Desorption experiment

The reused property of fabricated chelating membrane was evaluated via an adsorption/desorption process using 0.5 mol L⁻¹ of sulphuric acid (H₂SO₄) solution as the elution agent. The Pb(II)-saturated adsorbing membrane with a dry

weight of ~0.1 g was immersed in 200 mL of elution solution to release the adsorbed Pb(II), then the chelating membrane was immersed into 1 mmol L⁻¹ Pb(II) solution for the uptake of this metal again; this process was repeated 10 times to examine the reusability of the chelating membrane. The amounts of adsorbed and eluted Pb(II) during these tests were determined, and the desorption efficiency (DE) was calculated via Eq. (9) [41,42]:

$$\text{DE} = (q_1 / q_2) \times 100\% \quad (9)$$

where q_1 is the desorbed amount of Pb(II) from the membrane (mmol g⁻¹), while q_2 is the adsorbed amount of this metal (mmol g⁻¹) at equilibrium in the following adsorption process.

3. Results and discussion

3.1. Characterization of the chelating membrane

3.1.1. FE-SEM/EDS analysis

The surface and the cross-sectional morphologies of the PES-type chelating membrane (Figs. 3(a) and (b)) were characterized by SEM measurement, and the insets are those of aminated PES membrane (DETA-PES). Explicitly, both the chelating membrane and DETA-PES membrane have a uniform microporous surface structure. Base on the

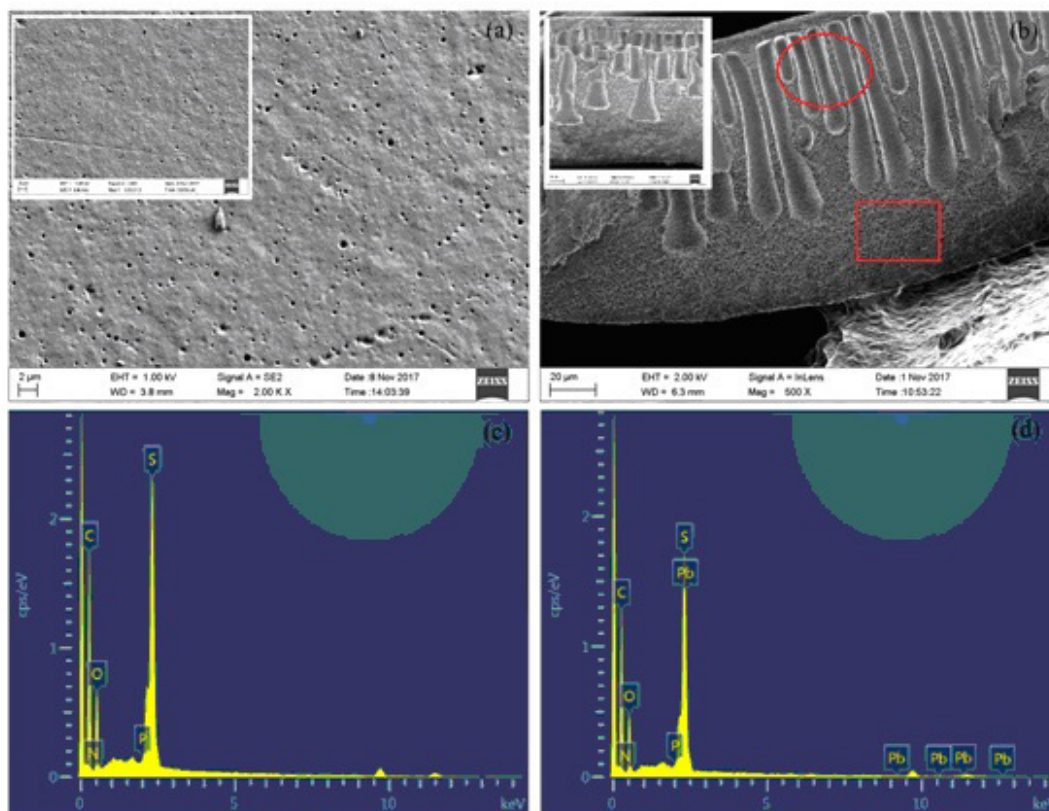


Fig. 3. FE-SEM and EDS of fabricated PES-type chelating membranes: (a) surface morphology; (b) cross-sectional morphology; (c) EDS spectrum before Pb(II) adsorption; (d) EDS spectrum after Pb(II) adsorption.

cross-sectional pictures (Fig. 3(b)), it can be seen that the finger-like pore structure near the surface (indicated by a circle) and the sponge-type structure (described using a rectangle) in the inner can be observed for these two membranes. This two-layered configuration will be helpful for the permeation of solution throughout the membrane and the reject of small-sized particles. The mean pore sizes for chelating membrane and DETA-PES membrane are 0.13 ± 0.02 and 0.15 ± 0.02 μm , and the determined pure water permeations of them are 660 ± 15 and 732 ± 21 $\text{L m}^{-2} \text{h}^{-1}$ at 0.1 MPa. Thus, the differences in structure and permeation flux between the above-mentioned two membranes are unremarkable.

Also, the EDS spectra of the chelating membrane before and after Pb(II) adsorption were recorded (Figs. 3(c) and (d)). Before the Pb(II) adsorption, elements of carbon, silicon, oxygen, sulfur and phosphorus are detected, inferring the aminophosphonation of PES molecular chain and the incorporation of aminophosphonic chelating group into this polymer matrix. Except for the above-mentioned elements, the lead element is also identified after the adsorption, which suggests that Pb(II) is captured by the chelating membrane from the solution.

3.1.2. FTIR spectra

The FTIR spectra of DETA-PES, and the fabricated chelating membranes before and after Pb(II) adsorption were measured and they are presented in Fig. 4. As indicated by Fig. 4(a), the three peaks at 1,150, 1,296 and 1,321 cm^{-1} are the symmetrical and asymmetrical stretching vibration peaks of the S=O functional group in PES molecular chain [27]; the stretching vibration peak between benzene ring and S atom locates at 1,103 cm^{-1} . The absorption peak at 1,656 cm^{-1} can be attributed to the stretching vibration of $-\text{NH}_2$ group [43], indicating that the DETA functional group is successfully grafted to the PES chain.

For the FTIR spectrum of chelating membrane (Fig. 4(b)), compared with Fig. 4(a), the absorption peak at 1,656 cm^{-1}

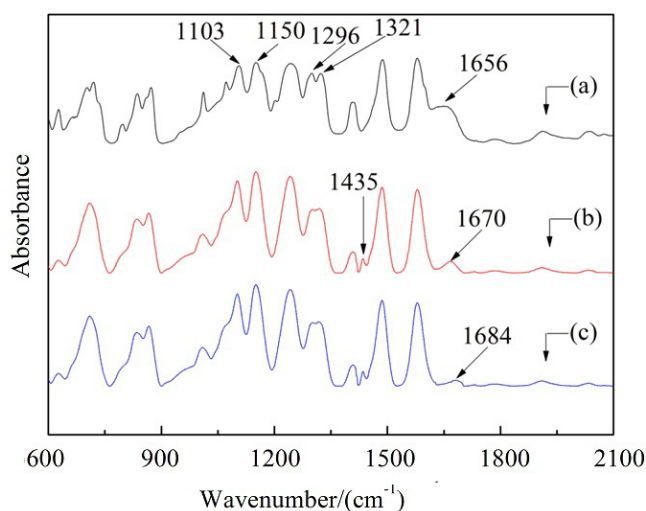


Fig. 4. FTIR of the fabricated membranes: (a) DETA-PES membrane; (b) chelating membrane before Pb(II) adsorption; (c) chelating membrane after Pb(II) adsorption.

almost disappears and a new absorption peak at 1,670 cm^{-1} can be observed, this peak is ascribed to plane bending of $-\text{OH}$ in phosphonic acid functional group [41,44,45]. In addition, another new absorption peak appearing at 1,435 cm^{-1} is detected, which can be identified to the stretching vibration model of P–C bond [41,46], thus suggesting incorporation of aminophosphonic acid group into the chelating membrane. After the Pb(II) uptake (Fig. 4(c)), the peak at 1,670 cm^{-1} shows a negative shift and its intensity also decreases somewhat, this may be due to the Pb(II) capture by the chelating membrane.

3.1.3. XPS analysis

The determined XPS spectra of the chelating membrane before and after Pb(II) adsorption are given in Fig. 5. For the spectra shown by Fig. 5(a), the peaks at binding energies of 27.2, 171.2, 235.2, 288, 134, 402.4 and 535.2 eV are attributable to O 2s, S 2p, S 2s, C 1s, P 2p, N 1s and O 1s, respectively. The presence of P 2p and N 1s validates the introduction of aminophosphonic acid chelating group. Based on the XPS measurement, for the chelating membrane, the atomic contents of detected elements are reported as follows: 72.9% for C, 18.65% for O, 3.96% for S, 3.02% for N, 1.47% for P. To take the ratios of N/S and P/S into view, the percent grafting of DETA and phosphonic acid could be calculated. The N/S and P/S ratios are 1.74 and 0.38, thus the grafting ratios of DETA and phosphoric acid anchored to PES molecular chains are 58% and 38%. After Pb(II) adsorption, the peaks related to Pb 4f can be identified except for above-mentioned six elements (Fig. 5(b)), indicating the capture of Pb(II) by the chelating membrane.

The high resolved N 1s spectra before and after adsorption of Pb(II) are shown in Figs. 5(c) and (d). Before Pb(II) adsorption, the peaks at 399.2, 400.3, and 400.5 eV are indicative of the existence of $-\text{NH}_2$, $-\text{NH}-$ and C–N groups [47,48], respectively. After the uptake of Pb(II), all intensities of these three peaks decrease. Additionally, the two peaks corresponding to $-\text{NH}_2$ and C–N groups shift to 399.6 and 400.7 eV. This can be due to the capture of Pb(II) by the membrane, that is, via the complexing interaction between this metal ion and N atoms in the chelating groups. The deconvoluted P 2p spectra before and after Pb(II) adsorption are shown in Figs. 5(e) and (f). Where, peaks with binding energies of 133.3 and 132.4 eV are attributed to P–O (P–OH and P=O) and P–C bonds [47,49]. After adsorption of Pb(II), there is no significant change in position and intensity for the P–C bond, thereby indicating that the P atom does not participate the chelating reaction. However, the binding energy of the P–O bond shifts to 133.6 eV, and its strength intensity also decreases, suggesting that the oxygen atoms in P–O take part in the capture of Pb(II) during the adsorption process.

3.2. Effects of basic variables

The effects of basic variables (pH, contact time, temperature, initial concentration of Pb(II)) on the adsorption of Pb(II) by the chelating membrane are illustrated in Fig. 6. As indicated by Fig. 6(a), it can be clearly seen that the Pb(II) uptake by the membrane rises ($1 < \text{pH} < 5.4$) and then decreases with the pH value beyond 5.4. At a low pH ($1 < \text{pH} < 4$), the

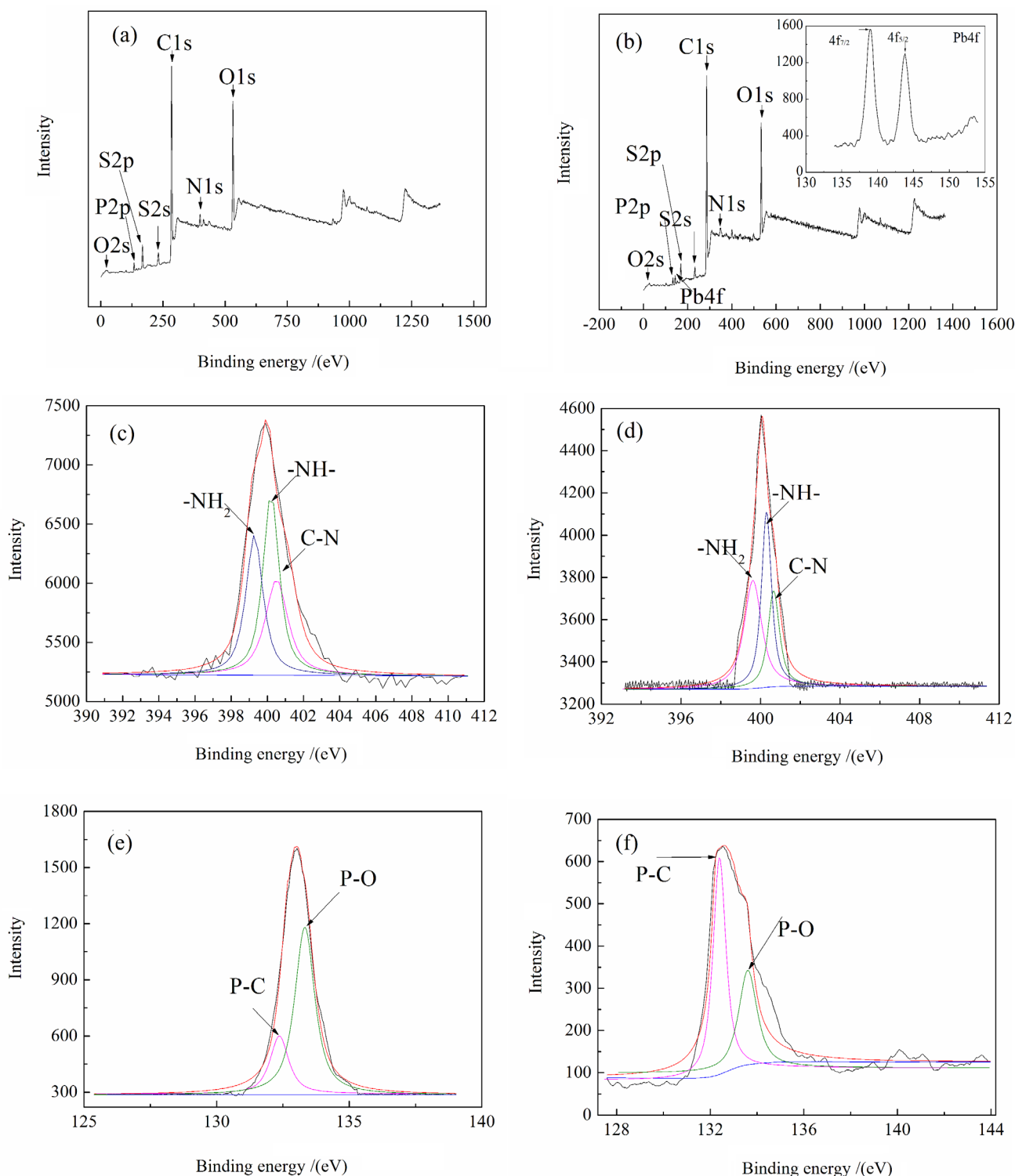


Fig. 5. XPS of the chelating membrane: (a) full spectrum before Pb(II) adsorption; (b) full spectrum after Pb(II) adsorption; (c) N 1s spectrum before Pb(II) adsorption; (d) N 1s spectrum after Pb(II) adsorption; (e) P 2p spectrum before Pb(II) adsorption; (f) P 2p spectrum after Pb(II) adsorption.

uptake of Pb(II) reduces due to a large amount of existent H^+ , which will inhibit the ionization of phosphonic acid functional group and reduce the chelating reaction between this chelating group and Pb(II). Also, H^+ can compete with Pb(II)

for occupying the active sites on the membrane. It can be seen from Fig. 6(b) when pH is higher than 6 but less than 7, a part of Pb(II) can change to $Pb(OH)^+$ and $[Pb_4(OH)_4]^{4+}$, the adsorption capacity of this metal also tends to decrease.

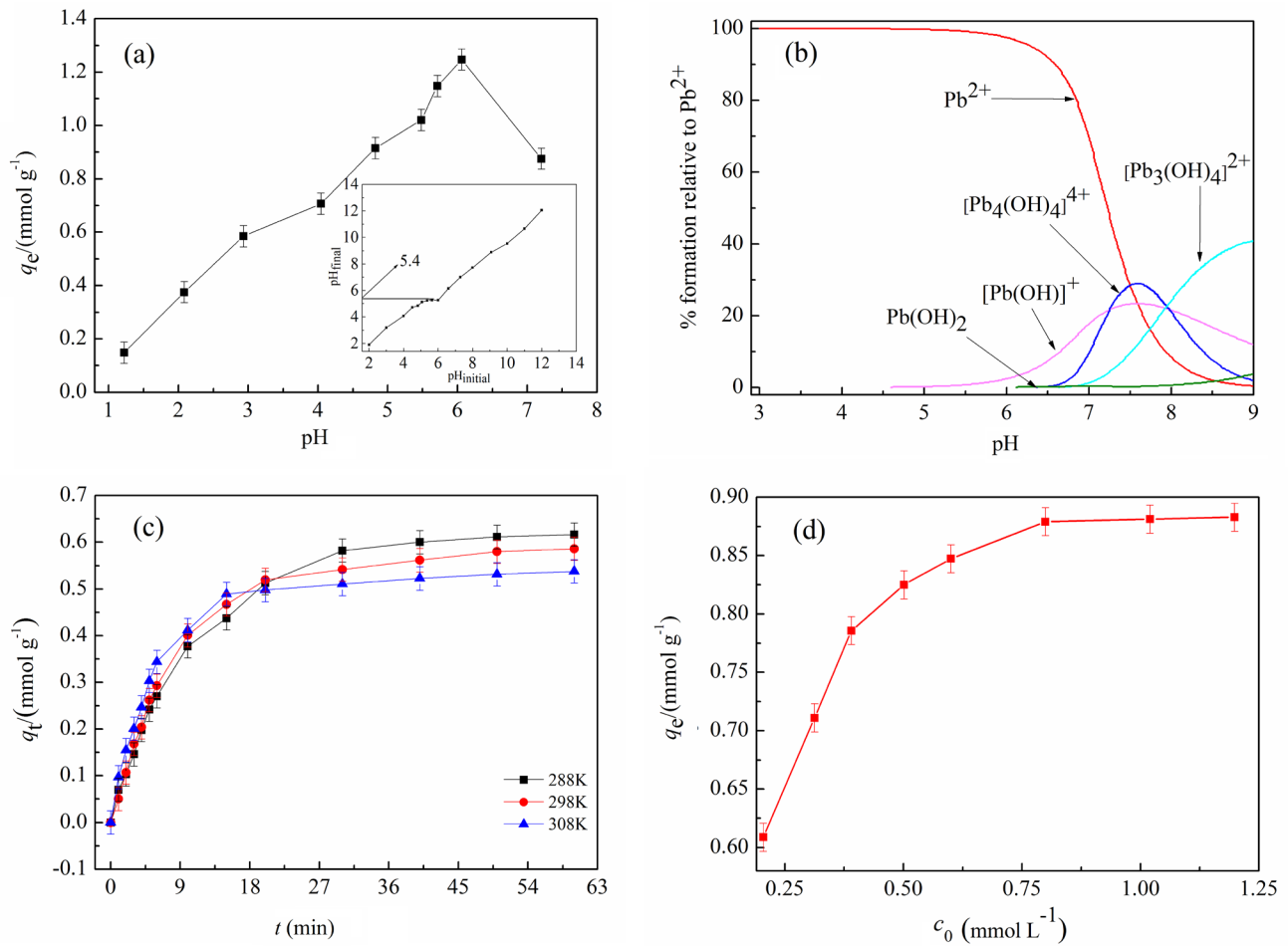


Fig. 6. Effects of pH, initial Pb(II) concentration, contact time and temperature (solution volume: 200 mL; membrane addition: ~0.1 g): (a) effect of pH ($c_0(\text{Pb(II)})$: 1.0 mmol L⁻¹; T : 298 K; t : 60 min); (b) form of Pb²⁺ in solution at different pH value; (c) effect of contact time and temperature ($c_0(\text{Pb(II)})$ = 1.0 mmol L⁻¹; pH: 5.4); (d) effect of initial Pb(II) concentration (T : 298 K; pH: 5.4; t : 60 min).

The conditions (pH > 7, and pH < 3) are not considered because the uptake of Pb(II) is not dominant at these conditions. As the pH value is in the range of 5–6, the competition of H⁺ is not prominent and the phosphonic acid group exists in the ionized form, which will be value for the capture of Pb(II). The optimized pH value for Pb(II) adsorption is 5.4, consistent with the determined pH_{pzc} (inset in Fig. 6(a)); the adsorption capacity of Pb(II) by the chelating membrane at this pH reaches the largest value (0.88 mmol g⁻¹).

It can be seen from Fig. 6(c) that the process of Pb(II) adsorption consists of two stages, namely the fast stage (first 10 min) and the slow stage (from 10 to 50 min). The adsorption rate increases rapidly in the first stage because there are available sites for the capture of Pb(II). On the other hand, in the following slow stage, the adsorption rate of Pb(II) uptake decreases due to the fact that most active sites on the surface and micropores are already occupied. In addition, the uptake of Pb(II) declines with the increase in temperature, indicating the exothermic nature of this adsorption process [50].

The influence of initial concentration of Pb(II) on its adsorption performance is presented in Fig. 6(d). The Pb(II) uptake at 298 K enhances with the increase in concentration of this metal, and it increases from 0.62 to 0.88 mmol g⁻¹ with

the concentration rising from 0.2 to 1.2 mmol L⁻¹. But the removal efficiency of Pb(II) reduces from 90% to 65%. Thus, the low temperature and small initial concentration of Pb(II) is beneficial to trap this pollutant from the solution.

3.3. Effects of the coexisting substances

For the adsorption process, the presence of coexistent substances can disturb the capture of model metal pollutant [51]. From the engineering perspective of discharge for lead-containing wastewater, herein, Cu(II), Ni(II) and Cd(II) three cations as well as CA, NTA and EDTA three complexing reagents were selected to describe effects of coexisting substances on the Pb(II) adsorption by the chelating membrane (Fig. 7), all concentrations of coexisting substances were from 0.2 to 1.2 mmol L⁻¹. Unquestionably, the coexisting cations and complexing reagents show an explicit interference on the Pb(II) uptake. With the increase in concentrations of three cations, the reduction in Pb(II) uptake becomes notable. The interfering order of them is: Cu(II) > Ni(II) > Cd(II). For instance, as the concentration of these three coexisting cations is 1.0 mmol L⁻¹, the Pb(II) uptake of the membrane decreases by 28% for Cu(II), 20% for Ni(II) and 11% for Cd(II).

The excessive CA, NTA and EDTA can be detected in effluent originated from the lead electroplating industry, and they always hinder the capture of Pb(II), and they always hinder the capture of Pb(II). Bearing a close resemblance to the cations, these three complexing agents also disturb the Pb(II) adsorption. As their concentration is 1.0 mmol L^{-1} , the Pb(II) uptake of the membrane decreases by 9% for CA, 23% for NTA and 41% for EDTA. Therefore, the negative effect of three complexing agents on the uptake of Pb(II) follows a trend of $\text{CA} < \text{NTA} < \text{EDTA}$. The disturbance of EDTA is higher than those of other two complexing agents. Although the presence of coexisting substances has an adverse effect on the Pb(II) uptake, the chelating membrane still can capture this metal pollutant, suggesting the fabricated PES-type chelating membrane competent for trapping Pb(II) from wastewater.

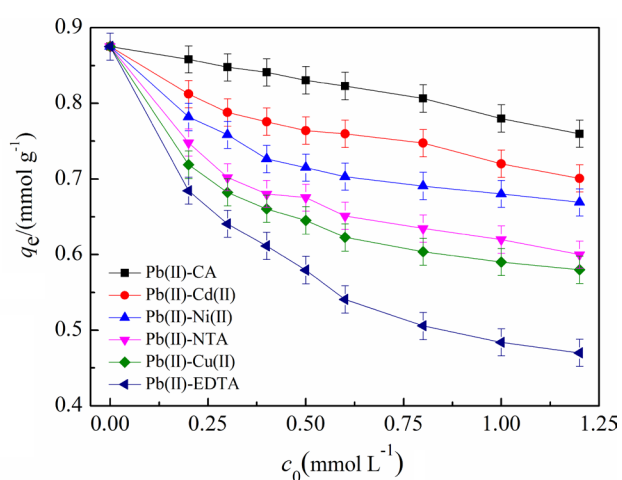


Fig. 7. Effect of coexisting substance concentration on the Pb(II) adsorption: $c_0(\text{Pb(II)}) = 1.0 \text{ mmol L}^{-1}$; $T: 298 \text{ K}$; $\text{pH}: 5.4$; membrane addition: $\sim 0.1 \text{ g}$; $t: 60 \text{ min}$; solution volume: 200 mL .

3.4. Studies of adsorption kinetics and adsorption isotherm

The adsorption kinetics and adsorption isotherms of Pb(II) uptake by the chelating membrane in the presence of Cu(II), Ni(II), Cd(II), CA, NTA and EDTA with a concentration of 1.0 mmol L^{-1} were studied at 298 K (Fig. 8); those of single Pb(II) system are presented in Fig. 6. The change in Pb(II) uptake with time was analyzed by pseudo-first-order and pseudo-second-order equations. As attested by Fig. 8(a), the coexistence of Cu(II), Ni(II) and Cd(II) interferes the adsorption of Pb(II) with a descending sequence of $\text{Cu(II)} > \text{Ni(II)} > \text{Cd(II)}$. Similarly, coexisting CA, NTA and EDTA also have a negative effect on the Pb(II) adsorption (Fig. 8(a)), and their interferences follow a trend of $\text{CA} < \text{NTA} < \text{EDTA}$.

Between the above-mentioned two adsorption kinetic equations, taking the coefficient of determination (R^2) into view, the pseudo-second-order adsorption equation ($R^2 > 0.99$) is more suitable than the pseudo-first-order adsorption equation for describing the process of Pb(II) adsorption. Therefore, the chemical adsorption may play a more important role in Pb(II) adsorption than physical adsorption [52]. The analyzed parameters of the pseudo-second-order model are listed in Table 1, where q_{eq} (mmol g^{-1}) is the equilibrium adsorption capacity, k_2 ($\text{g min}^{-1} \text{mmol}^{-1}$) is the rate constant, RMSE is root mean square error and χ^2 is the chi-squared distribution. By comparison of k_2 , it can be deduced that competitive adsorption between Pb(II) and three coexisting cations accelerates the adsorption process. In addition, for the three complexing agent coexisting systems, k_2 follows an increasing order: $\text{single Pb(II)} < \text{Pb(II)-CA} < \text{Pb(II)-NTA} < \text{Pb(II)-EDTA}$, which indicates the coexisting complexing agents exert an interference on the Pb(II) uptake; among them, the adverse effect of EDTA is the most significant.

Herein, three adsorption isotherm models of Freundlich, Langmuir and Dubinin–Radushkevich (D-R) were used to analyze the adsorption isotherm data for aforesaid seven systems. It is very similar to the case of adsorption kinetics

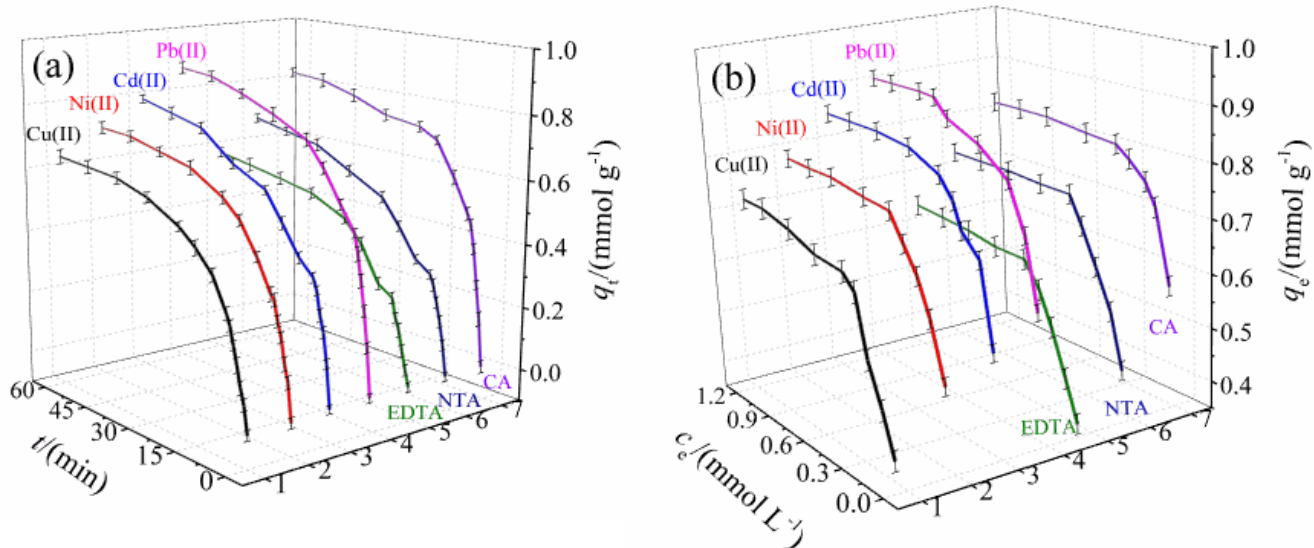


Fig. 8. Adsorption kinetics and adsorption isotherm for Pb(II) onto the chelating membrane ($c_0(\text{Cu(II)}) = c_0(\text{Ni(II)}) = c_0(\text{Cd(II)}) = c_0(\text{CA}) = c_0(\text{NTA}) = c_0(\text{EDTA}) = 1.0 \text{ mmol L}^{-1}$; $T: 298 \text{ K}$; $\text{pH}: 5.4$; membrane addition: $\sim 0.1 \text{ g}$; solution volume: 200 mL): (a) adsorption kinetics ($c_0(\text{Pb(II)}) = 1.0 \text{ mmol L}^{-1}$); (b) adsorption isotherm (time: 60 min).

Table 1
Analyzed parameters of pseudo-second-order and Langmuir models for the chelating membrane toward Pb(II) at 298 K

Models	Parameters	Systems						
		Single Pb(II)	Pb(II)-Cd(II)	Pb(II)-Ni(II)	Pb(II)-Cu(II)	Pb(II)-CA	Pb(II)-NTA	Pb(II)-EDTA
Pseudo-second-order $q_t = \frac{k_2 q_{et}^2 t}{1 + k_2 q_{et} t}$	q_{et} (mmol g ⁻¹)	0.97±0.02	0.89±0.02	0.81±0.01	0.73±0.01	0.90±0.02	0.78±0.01	0.69±0.01
	k_2 (g min ⁻¹ mmol ⁻¹)	0.20±0.01	0.17±0.01	0.17±0.01	0.18±0.01	0.23±0.02	0.27±0.01	0.28±0.02
	R^2	0.998	0.998	0.998	0.998	0.992	0.999	0.991
	RMSE	0.013	0.013	0.009	0.010	0.025	0.007	0.020
	χ^2	2E-4	1E-4	1E-4	6E-4	4E-5	4E-4	2E-4
Langmuir $q_e = \frac{q_m K_L c_e}{1 + K_L c_e}$	q_m (mmol g ⁻¹)	0.92±0.01	0.86±0.01	0.81±0.01	0.79±0.02	0.82±0.01	0.789±0.01	0.704±0.02
	K_L (L mmol ⁻¹)	38.976±3.764	32.261±3.786	30.684±3.483	11.342±1.472	29.604±2.010	17.564±1.853	11.327±1.298
	R^2	0.964	0.953	0.952	0.949	0.971	0.962	0.956
	RMSE	0.021	0.023	0.022	0.028	0.014	0.021	0.021
	χ^2	4E-4	5E-4	5E-4	8E-4	1.9E-2	4E-4	4E-4

(Fig. 8(b)), the coexistence of the cations and complexing agents reduces the uptake of Pb(II). Among aforesaid three models, the Langmuir model is more applicable than two others for describing this isotherm adsorption process. Also, the analyzed parameters of Langmuir model are listed in Table 1, where q_m (mmol g⁻¹) is the maximum adsorption capacity and K_L (L mmol⁻¹) is the Langmuir adsorption constant. The obtained q_m is slightly greater than the experimental value because some active sites on the membrane surface are not occupied. The value of K_L related to the affinity to Pb(II) for above-mentioned three cations coexisting systems follows an order of Pb(II)-Cd(II) > Pb(II)-Ni(II) > Pb(II)-Cu(II), thereby suggesting the interference of Cu(II) is higher than those of Cd(II) and Ni(II). Also, based on the value of K_L for three complexing agents coexisting systems, it can be inferred that the interferences of three complexing agents follow the trend of EDTA > NTA > CA. Although analyzed parameters for both Freundlich and D-R models are not shown, their characteristics are briefly described as follows: the obtained Freundlich parameter of $1/n$ corresponding to adsorption intensity is smaller than 1, indicating the easy occurrence of Pb(II) adsorption. The average free energy of adsorption derived from D-R model ranges from 14.43 to 23.57 kJ mol⁻¹, suggesting the chemisorption feature of Pb(II) adsorption [53].

In addition, three thermodynamic parameters, that is, standard free energy change (ΔG°), standard enthalpy change (ΔH°) and standard entropy change (ΔS°) at 298 K were also calculated to reveal the adsorption characteristics of Pb(II) adsorption by the chelating membrane. These three parameters were calculated by Eqs. (10)–(12) [54]:

$$K_D = K_L \quad (10)$$

$$\ln K_D = -\frac{\Delta H^\circ}{RT} + \frac{\Delta S^\circ}{R} \quad (11)$$

$$\Delta G^\circ = \Delta H^\circ - T\Delta S^\circ \quad (12)$$

where K_D is the distribution coefficient (L mol⁻¹), R is the gas constant (J mol⁻¹ K⁻¹) and T is the temperature (K). The obtained ΔH° values for single Pb(II), Pb(II)-Cu(II), Pb(II)-Ni(II), Pb(II)-Cd(II), Pb(II)-CA, Pb(II)-NTA and Pb(II)-EDTA systems are -81.68, -81.05, -72.78, -75.90, -79.64, -82.13, -78.53 kJ mol⁻¹, thus illustrating the process of Pb(II) capture being an exothermic reaction. The obtained ΔG° at 298 K is that: -23.30 for single Pb(II), -22.67 for Pb(II)-Cu(II), -22.39 for Pb(II)-Ni(II), -20.51 for Pb(II)-Cd(II), -22.98 for Pb(II)-CA, -21.13 for Pb(II)-NTA and -20.18 kJ mol⁻¹ for Pb(II)-EDTA system, verifying that the Pb(II) adsorption process exhibits a spontaneous nature [54,55]. The negative ΔS° (in the range of -0.16 to -0.21 kJ mol⁻¹ K⁻¹) shows an decrease in the randomness of the adsorption system, this may be because the water-unoccupying sites at Pb(II) are occupied by the oxygen and nitrogen atoms in aminophosphonic acid groups.

3.5. Comparison of the uptake of Pb(II)

As the initial Pb(II) concentration, pH, adsorption time and temperature were kept at 1 mmol L⁻¹, 5.4, 60 min and

298 K, respectively, the uptakes of this metal by pristine PES, DETA-PES and the chelating membranes are depicted in Fig. 9. It can be seen that the pristine PES membrane almost cannot trap Pb(II), the ability of fabricated chelating membrane for the Pb(II) capture is superior to that of DETA-PES membrane. The Pb(II) uptake of fabricated chelating membrane is more one-order magnitude of level than that of DETA-PES membrane.

The Pb(II) uptakes of some reported adsorbents are reported in Table 2 [56–65]. By comparison of the data of Pb(II) uptake, the fabricated PES-type chelating membrane shows an excellent property in the capture of Pb(II). Besides the high affinity to Pb(II), the chelating membrane can capture other metals (such as Cu(II) and Ni(II)). Therefore, this fabricated chelating membrane will be competent for the removal of toxic metals from industrial effluents.

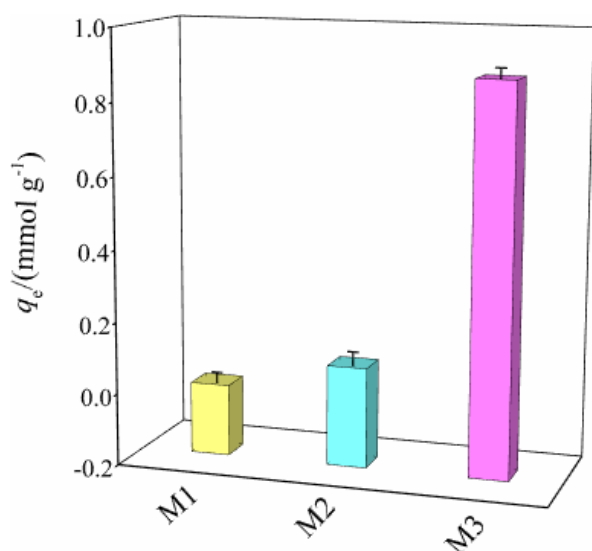


Fig. 9. Pb(II) uptake of pristine PES (M1), DETA-PES membrane (M2) and the chelating membrane (M3): $c_0(\text{Pb(II)}) = 1.0 \text{ mmol L}^{-1}$; T : 298 K; pH: 5.4; membrane addition: $\sim 0.1 \text{ g}$; t : 60 min; solution volume: 200 mL.

3.6. Continuous adsorption studies

3.6.1. Effects of flow rate and thickness of membrane stack

The effect of flow rate on the adsorption of Pb(II) by the membrane stack with a thickness of 0.36 mm is shown in Fig. 10(a). The adsorption capacity of the membrane reduces with the increase in flow rate, this can be due to the fact that the residence time of Pb(II) in the membrane stack will shorten with the increase in flow rate, and there is not enough time to capture Pb(II), thus resulting in the decrease in the uptake of this metal. Taking the result shown by Fig. 10(a) into account, the flow rate of 0.46 cm min^{-1} is selected for other adsorption tests.

In addition, the effect of membrane stack thickness on the Pb(II) uptake is given in Fig. 10(b). At the conditions of same flow rate and initial concentration of Pb(II), due to the polyaminophosphonic acid groups uniformly distribute on surface and inner side of the membrane, three membrane stacks (with thicknesses of 0.18, 0.36 and 0.72 mm) exhibit a similar affinity to Pb(II), thus the discrepancy in the Pb(II) uptake is unremarkable and can be ignored in some extent. But at the beginning of Pb(II) adsorption, a thin thickness will be slightly helpful to the increase in metal uptake, this may be due to the light weight of membrane stack. The membrane stack with a thickness of 0.36 mm was employed to study the following study.

3.6.2. Analysis of breakthrough curves

The breakthrough curves of three membrane stacks with thicknesses of 0.18, 0.36 and 0.72 mm were obtained for the single Pb(II) and six coexisting systems (Pb(II)-Cu(II), Pb(II)-Ni(II), Pb(II)-Cd(II), Pb(II)-CA, Pb(II)-NTA and Pb(II)-EDTA) (Fig. 11), with the concentrations of all substances kept at 1 mmol L^{-1} and the flow rate at 0.46 cm min^{-1} . The determined TMP of membrane stack increases with the increase in thickness of the membrane stack, for instance, the TMP value is 0.19 MPa for $Z = 0.18 \text{ mm}$, 0.31 MPa for $Z = 0.36 \text{ mm}$, and 0.45 MPa for $Z = 0.72 \text{ mm}$. However, for the above-mentioned seven systems with the same membrane-stacked thickness, the difference in TMP is inconspicuous.

Table 2
Comparison in Pb(II) uptake of different adsorbents

Adsorbent	Test condition					Pb(II) uptake (mg g^{-1})	Refs.
	pH	Pb(II) concentration (mmol L^{-1})	Temperature (K)	Time (h)	Adsorbent addition (g L^{-1})		
PES-type chelating membrane	5.4	1.0	298	1	0.5	291	This test
Novel chitosan	5.0	0.6	298	24	1	297	[56]
LS-GO-PANI	5.0	0.6	303	24	1.6	216	[57]
SMA	3.0	1.06	298	2	4	143	[58]
Chitosan nanofibrils	5.0	0.6	293	4	0.5	118	[59]
Pb(II)-imprinted silica	4.5	2.9	298	1	4	62	[60]
Tourmaline	5.0	0.3	298	50	2	108	[61]
Bromoacetylated apple seeds	4.0	5	298	24	0.5	523	[62]
MDA- Fe_3O_4	5.0	0.33	303	1.5	0.49	333	[63]
Activated carbon	6.0	0.48	303	1	0.35	23	[64]
$\text{SiO}_2/\text{graphene}$	4.5	0.06	298	1	0.3	114	[65]

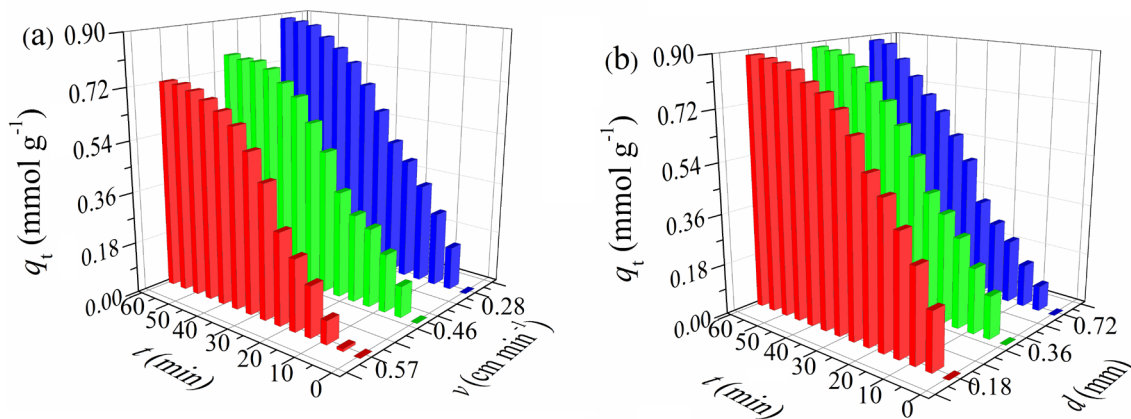


Fig. 10. Effects of flow rate and thickness of membrane stack on Pb(II) uptake: (a) flow rate ($c_0(\text{Pb(II)}) = 1 \text{ mmol L}^{-1}$; thickness of membrane stack: 0.36 mm; $T: 298 \text{ K}$; $\text{pH}: 5.4$); (b) thickness of membrane stack ($c_0(\text{Pb(II)}) = 1 \text{ mmol L}^{-1}$; $v: 0.46 \text{ cm min}^{-1}$; $T: 298 \text{ K}$; $\text{pH}: 5.4$).

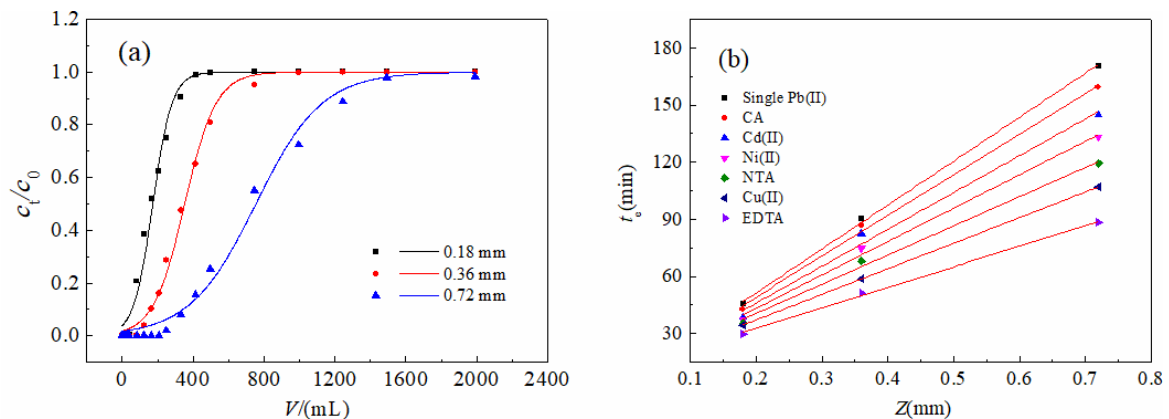


Fig. 11. Tested breakthrough curve of Pb(II) adsorption by the chelating membrane and the fitted curves by BDST model: ($c_0(\text{Pb(II)}) = 1.0 \text{ mmol L}^{-1}$; $T: 298 \text{ K}$; $v: 0.46 \text{ cm min}^{-1}$; $\text{pH}: 5.4$; $Z = 0.18, 0.36, 0.72 \text{ mm}$): (a) tested breakthrough curves; (b) fitted curves by BDST model ($c_0(\text{Cu(II)}) = c_0(\text{Ni(II)}) = c_0(\text{Cd(II)}) = c_0(\text{CA}) = c_0(\text{NTA}) = c_0(\text{EDTA}) = 1.0 \text{ mmol/L}$).

At the initial time, when the Pb(II)-containing feed was bumped through the membrane stack, the Pb(II) concentration in effluent cannot be detected. This is due to the effect of Pb(II) capture by the sufficient unoccupied sites in the membrane stack. With the extension of filtration time, more and more aminophosphonic acid groups anchored on the active sites are chelated by Pb(II), and the amount of unoccupied sites decreases, so the concentration of Pb(II) in effluent slightly increases; this process is usually named the breakthrough of membrane stack. After that, the Pb(II) concentration in effluent rises drastically until it reaches a stable value, which corresponds to the absolute breakthrough of membrane stack. The breakthrough time (t_b , the position at $c/c_0 = 0.05$) and the exhaustion time (t_e , the position at $c/c_0 = 0.95$) [41] are prolonged with the increase in thickness, this is interpreted as follows: for the single Pb(II) system, as Z rises from 0.18 mm to 0.36 and 0.72 mm, t_b extends from 6.19 min to 12.22 and 25.08 min; accordingly, t_e prolongs from 45.35 min to 90.47 and 170.55 min. Compared with the single Pb(II) system, t_b and t_e for other six coexisting systems decrease, showing the disturbances of the coexisting cations and complexing agents. When the thickness of membrane stack is 0.36 mm, compared t_b and

t_e of six coexisting systems with those of single Pb(II) system, t_b and t_e decrease to 8.09 and 58.8 min for Pb(II)-Cu(II), 9.28 and 75 min for Pb(II)-Ni(II), 11.16 and 82.28 min for Pb(II)-Cd(II), 10.22 and 86.83 min for Pb(II)-CA, 8.54 and 68.12 min for Pb(II)-NTA, 7.23 and 51.18 min for Pb(II)-EDTA. Among the coexisting cations and complexing reagents, the disturbances of Cu(II) and EDTA on the Pb(II) uptake are the most notable.

The obtained S-type breakthrough curves hints that the BDST model will be applicable for the analysis of experimental data [66], and the analyzed parameters of this model are reported in Table 3. Taking the coefficient of determination ($R^2 > 0.99$) into view, it can be confirmed that BDST model is suitable for describing the breakthrough process. By comparison of obtained K_a values for the single Pb(II) system and these six coexisting systems with the same thickness of membrane stack, for the single Pb(II) system, the larger K_a suggests that a thin membrane stack can avoid the breakthrough [66]. While, for the six coexisting systems mentioned earlier, the thicker membrane stack should be required to avoid the occurrence of breakthrough. The needed thickness of membrane stacks follows an order of Pb(II)-EDTA > Pb(II)-Cu(II) > Pb(II)-NTA > Pb(II)-Ni(II) > Pb(II)-Cd(II) > Pb(II)-CA > single Pb(II).

3.7. Analysis of PDEs

3.7.1. Result of PDEs analysis

As a matter of fact mentioned earlier, among the coexisting cations and complexing reagents, the disturbing effects of Cu(II) and EDTA on the Pb(II) uptake are most remarkable. Thus, the negative influences of Cu(II) and EDTA on the distribution of Pb(II) along the depth direction of membrane stack were evaluated. The analyzed results of PDEs for

single Pb(II), Pb(II)-Cu(II) and Pb(II)-EDTA systems with a membrane stack thickness of 0.36 mm are shown in Fig. 12. As indicated by Figs. 12(a)–(c), there are Pb(II) concentration gradients for all above-mentioned three systems, that is, the Pb(II) uptake shows a decreasing trend along the depth direction of membrane stack. This can be explained that the Pb(II) concentration of influent becomes lower as the solution contacts the underpart of membrane stack due to the capture of this metal by upside membrane matrix, thus resulting in

Table 3
Analyzed parameters of BDST model for Pb(II) adsorption by the chelating membrane at 298 K

System	Z (mm)	t_b (min)	t_e (min)	BDST model				
				N_0 (mmol L ⁻¹)	K_a (L min ⁻¹ mmol ⁻¹)	R^2	RMSE	χ^2
Single Pb(II)	0.18	6.19	45.35	1,060.29±32.12	0.55±0.05	0.998	2.72	7.37
	0.36	12.22	90.47					
	0.72	25.08	170.55					
Pb(II)-CA	0.18	5.21	42.64	985.05±49.95	0.46±0.04	0.995	4.22	17.83
	0.36	10.22	86.83					
	0.72	20.02	159.41					
Pb(II)-Cd(II)	0.18	5.34	38.63	889.66±78.22	0.40±0.02	0.985	6.61	43.72
	0.36	11.16	82.28					
	0.72	21.96	144.84					
Pb(II)-Ni(II)	0.18	4.96	37.34	806.23±54.10	0.36±0.01	0.991	4.17	20.91
	0.36	9.28	75					
	0.72	19.05	133.21					
Pb(II)-NTA	0.18	4.24	35.55	704.81±44.17	0.30±0.01	0.992	3.73	13.94
	0.36	8.54	68.12					
	0.72	17.06	119.29					
Pb(II)-Cu(II)	0.18	3.95	34.47	617.27±1.55	0.28±0.02	0.999	0.13	0.02
	0.36	8.09	58.8					
	0.72	16.25	106.97					
Pb(II)-EDTA	0.18	3.46	29.8	495.79±17.52	0.26±0.02	0.996	1.48	2.19
	0.36	7.23	51.18					
	0.72	14.65	88.4					

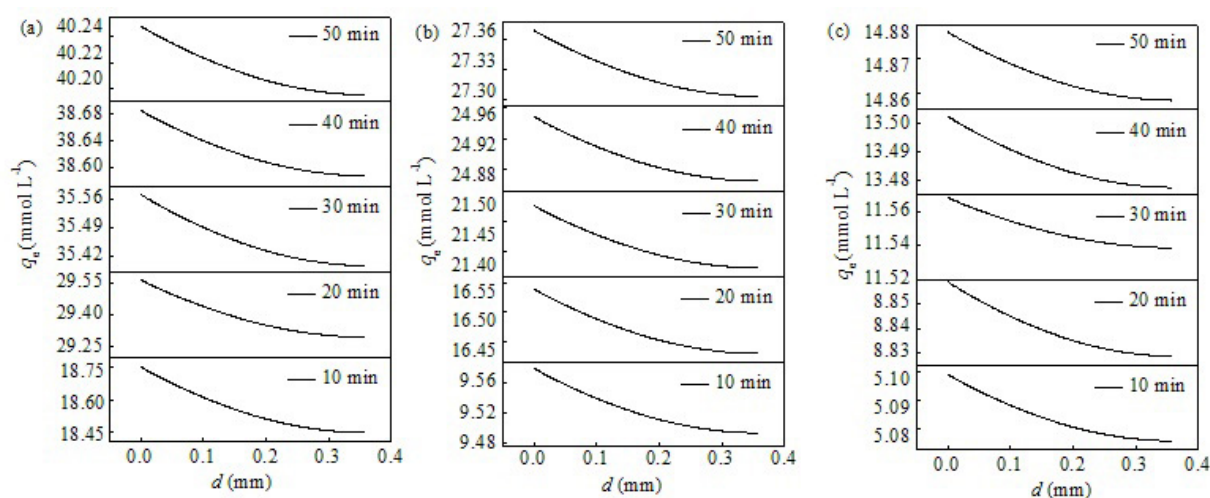
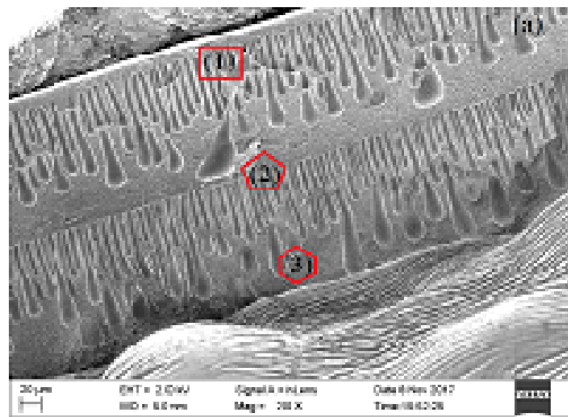


Fig. 12. PDEs analyzed data for captured Pb(II) concentration on the membrane stack: (a) single Pb(II) system; (b) Pb(II)-Cu(II) system; (c) Pb(II)-EDTA system.

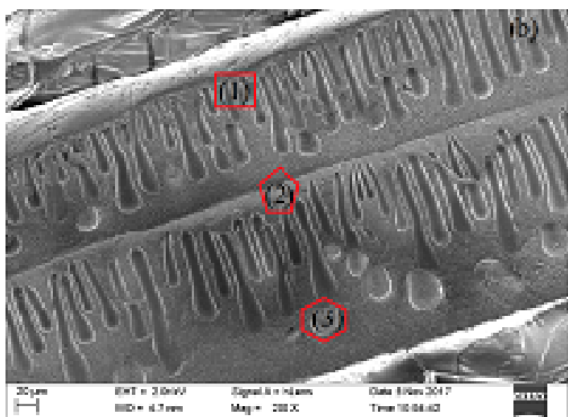
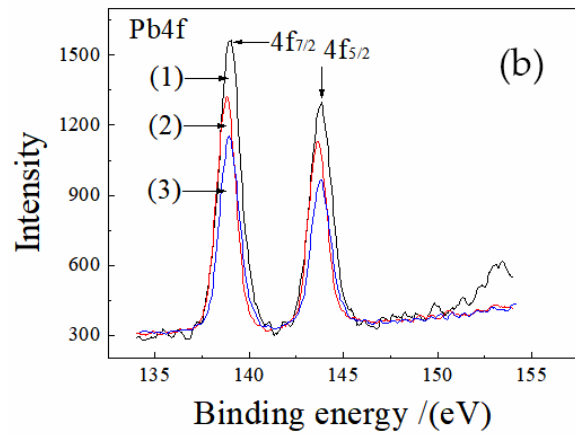
the decrease of Pb(II) uptake. At the fixed position along the depth direction of membrane stack, the captured amount of Pb(II) at this point rises with the filtration time increasing. But it follows a descending order of single Pb(II) > Pb(II)-Cu(II) > Pb(II)-EDTA, also suggesting the interferences of Cu(II) and EDTA. Of course, EDTA shows a more detrimental effect than Cu(II) on the Pb(II) uptake.

3.7.2. Validated results of SEM and XPS

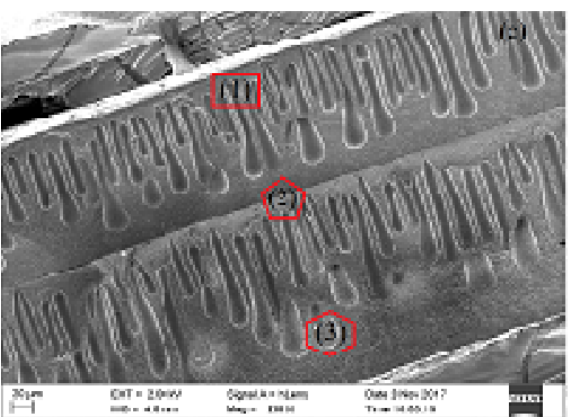
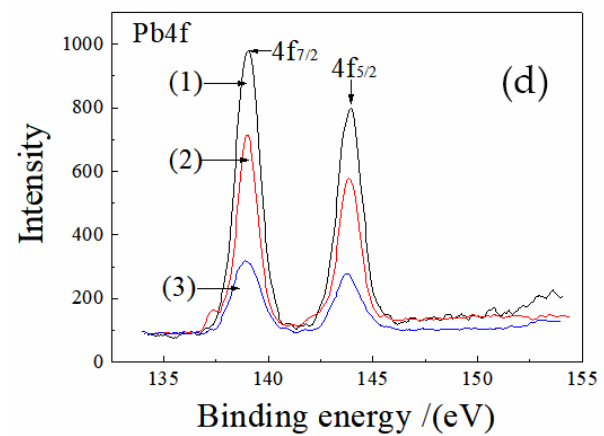
The analyzed results of PDEs for the above-mentioned three systems were validated by SEM and XPS measurement (Fig. 13). The results of SEM are shown in Figs. 13(a), (c) and (e), and the XPS spectra of Pb(II) in Figs. 13(b), (d) and (f). There are three labeled positions (1, 2 and 3)



(a)



(c)



(e)

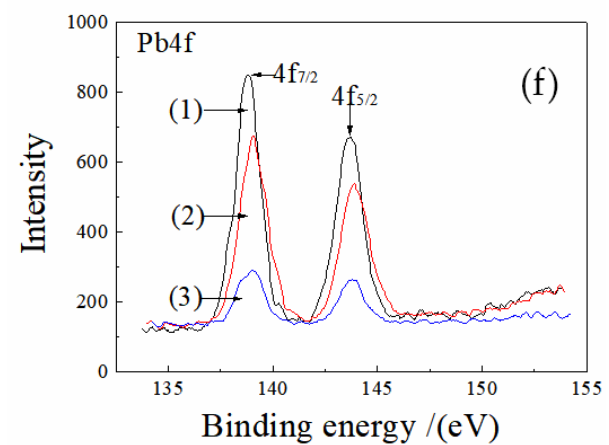


Fig. 13. Validated results for PDEs analysis by SEM and XPS measurements: ((a) and (b)) single Pb(II) system; ((c) and (d)) Pb(II)-Cu(II) system; ((e) and (f)) Pb(II)-EDTA system.

Table 4
Determined Pb(II) content (at%) by EDS and XPS

Position	EDS			XPS		
	Single Pb(II)	Pb(II)-Cu(II)	Pb(II)-EDTA	Single Pb(II)	Pb(II)-Cu(II)	Pb(II)-EDTA
1	4.1	2.4	2	3.6	2.1	1.8
2	3.5	2	1.4	3.1	1.5	1.4
3	2.9	1.5	0.8	2.6	0.9	0.8

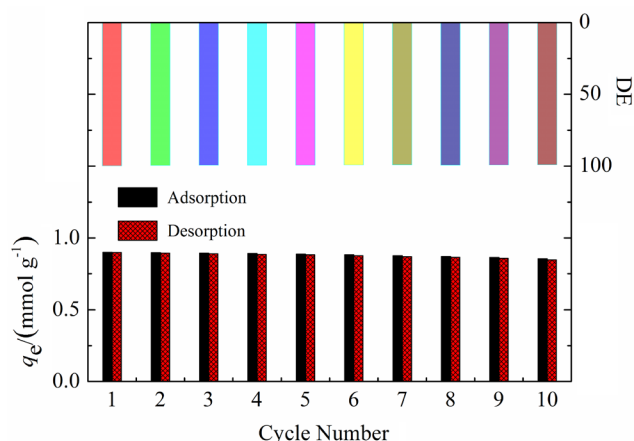


Fig. 14. Regeneration performance of the chelating membrane.

employed to assess the Pb(II) distribution along the depth direction. Positions 1, 2 and 3 are, approximately, close to the top, middle and bottom of the membrane stack, respectively. The determined Pb(II) contents by EDS and XPS measurements at these three positions for single Pb(II), Pb(II)-Cu(II) and Pb(II)-EDTA three systems are tabulated in Table 4. Compared with the Pb 4f spectra for each system, the intensity of Pb 4f follows an increasing trend of position 3 < position 2 < position 1. At the same position, the intensity of this metal for the above-mentioned three systems is in the sequence: single Pb(II) system > Pb(II)-Cu(II) > Pb(II)-EDTA. Unambiguously, the results in Fig. 13 and Table 4 confirm the presence of concentration gradient for Pb(II) along the depth direction (namely, the Pb(II) uptake decreases with the extension in depth of membrane stack); also the interferences of Cu(II) and EDTA are validated. These results are perfectly consistent with the results of PDEs.

3.8. Reused property of the chelating membrane

Lastly, the reused property of fabricated PES-type chelating membrane was evaluated; herein, 0.5 mol L⁻¹ of H₂SO₄ solution was employed to regenerate this chelating membrane. The adsorption/desorption processes were performed 10 times (Fig. 14). After 10 turns of adsorption/desorption processes, the Pb(II) uptake still exceeds 0.8 mmol g⁻¹ and its loss is less than 10%, so the adsorption capacity of the membrane is well maintained. In addition, DE of the membrane is larger than 95%. Based on this result, the fabricated PES-type chelating membrane can be repeatedly used for the removal of Pb(II) from the aqueous solution.

4. Conclusions

A PES-type chelating membrane bearing the aminophosphonic acid functional groups was fabricated and employed to capture Pb(II) from aqueous solution via an adsorption process. The adsorption characteristics of Pb(II) by the chelating membrane with the presence of coexisting Cu(II), Ni(II), Cd(II), CA, NTA and EDTA were studied. The capture performance of this metal by the chelating membrane was evaluated by a continuous filtration test. The concentration distribution of Pb(II) along the depth direction of membrane stack was also evaluated. In addition, the reused property of this membrane was assessed. The conclusions are shown as follows:

- (1) The coexisting cations and complexing reagents interfere with the Pb(II) adsorption onto the chelating membrane. The disturbance of three cations follows an order of Cu(II) > Ni(II) > Cd(II). For the three complexing reagents, the detrimental effect of EDTA on the Pb(II) uptake is much higher than that of CA and NTA.
- (2) The coexisting cations and complexing reagents decrease the Pb(II) uptake, but they do not alter the Pb(II) adsorption nature of the chelating membrane. The pseudo-second-order equation and the Langmuir model are applicable to describe the adsorption kinetics and the adsorption isotherms, respectively. The uptake of Pb(II) is a spontaneous and exothermic process. Also, the chelating membrane shows an excellent reused property, suggesting a potential application in recovery of Pb(II) from the aqueous solution.
- (3) Based on the PDEs analysis and following EDS and XPS verifications, the concentration gradient of Pb(II) along the direction of axial filtration depth is identified, that is, the captured Pb(II) on the membrane stack decreases with the extension of filtration depth.

Acknowledgment

This work was supported by the Hebei Provincial Natural Science Foundation of China (Grant No. B2016203012).

References

- [1] G.Y. Zhou, J.M. Luo, C.B. Liu, L. Chu, J. Crittenden, Efficient heavy metal removal from industrial melting effluent using fixed-bed process based on porous hydrogel adsorbents, *Water Res.*, 131 (2018) 246–254.
- [2] I. Vergilia, Z.B. Göndera, Y. Kaya, G. Gürdağ, S. Cavus, Sorption of Pb (II) from battery industry wastewater using a weak acid cation exchange resin, *Process Saf. Environ. Prot.*, 107 (2017) 498–507.

- [3] H.F. Wen, C. Yang, D.G. Yu, X.Y. Li, D.F. Zhang, Electrospun zein nanoribbons for treatment of lead-contained wastewater, *Chem. Eng. J.*, 290 (2016) 263–272.
- [4] M. Aliabadi, M. Irani, J. Ismaeili, H. Piri, M.J. Parnian, Electrospun nanofiber membrane of PEO/chitosan for the adsorption of nickel, cadmium, lead and copper ions from aqueous solution, *Chem. Eng. J.*, 220 (2013) 237–243.
- [5] M.M. Matthew, S.H. Brock, A.A. David, Chemical precipitation of heavy metals from acid mine drainage, *Water Res.*, 36 (2002) 4757–4764.
- [6] K.A. Vo, X.J. Xu, T.G. Li, R.H. Peng, S.L. Liu, X.L. Yue, Research on a new electrochemical method combined with chemical coagulation in removal of lead, zinc, and copper from wastewater, *Desal. Wat. Treat.*, 57 (2016) 15343–15352.
- [7] P. Kumar, A. Pournara, K.H. Kim, V. Bansal, S. Rapti, M.J. Manos, Metal-organic frameworks: challenges and opportunities for ion-exchange/sorption applications, *Prog. Mater. Sci.*, 86 (2017) 25–74.
- [8] T. Robinson, Removal of toxic metals during biological treatment of landfill leachates, *Waste Manage.*, 63 (2017) 299–309.
- [9] B.A.M. Al-Rashdi, D.J. Johnson, N. Hilal, Removal of heavy metal ions by nanofiltration, *Desalination*, 315 (2013) 2–17.
- [10] E. Asuquo, A. Martin, P. Nzerem, F. Siperstein, X.L. Fan, Adsorption of Cd(II) and Pb(II) ions from aqueous solutions using mesoporous activated carbon adsorbent: equilibrium, kinetics and characterisation studies, *J. Environ. Chem. Eng.*, 5 (2017) 679–698.
- [11] K. Singh, M. Gautam, B. Chandra, A. Kumar, Removal of Pb(II) from its aqueous solution by activated carbon derived from Balam Khira (*Kigelia africana*), *Desal. Wat. Treat.*, 57 (2016) 24487–24497.
- [12] J.J. Keating, J. Imbrogno, G. Belfort, Polymer brushes for membrane separations: a review, *ACS Appl. Mater. Interfaces*, 8 (2016) 28383–28399.
- [13] Y. Cui, Q. Ge, X.Y. Liu, T.S. Chung, Novel forward osmosis process to effectively remove heavy metal ions, *J. Membr. Sci.*, 467 (2014) 188–194.
- [14] M.A. Khosa, S.S. Shah, X.S. Feng, Metal sericin complexation and ultrafiltration of heavy metals from aqueous solution, *Chem. Eng. J.*, 244 (2014) 446–456.
- [15] M. Nemati, S.M. Hosseini, M. Shabaniyan, Novel electrodialysis cation exchange membrane prepared by 2-acrylamido-2-methylpropane sulfonic acid; heavy metal ions removal, *J. Hazard. Mater.*, 337 (2017) 90–104.
- [16] G.Y. Zeng, Y. He, Y.Q. Zhan, L. Zhang, Y. Pan, C.L. Zhang, Z.X. Yu, Novel polyvinylidene fluoride nanofiltration membrane blended with functionalized halloysite nanotubes for dye and heavy metal ions removal, *J. Hazard. Mater.*, 317 (2016) 60–72.
- [17] Y.F. Huang, D.H. Wu, X.D. Wang, W. Huang, D. Lawless, X.S. Feng, Removal of heavy metals from water using polyvinylamine by polymer-enhanced ultrafiltration and flocculation, *Sep. Purif. Technol.*, 158 (2016) 124–136.
- [18] D. Kotodyńska, Z. Hubicki, Comparison of chelating ion exchange resins in sorption of copper(II) and zinc(II) complexes with ethylenediaminetetraacetic acid (EDTA) and nitrilotriacetic acid (NTA), *Can. J. Chem.*, 86 (2008) 958–969.
- [19] H. Chen, J.H. Lin, N. Zhang, L.Z. Chen, S.P. Zhong, Y. Wang, W.G. Zhang, Q.D. Ling, Preparation of MgAl-EDTA-LDH based electrospun nanofiber membrane and its adsorption properties of copper(II) from wastewater, *J. Hazard. Mater.*, 345 (2018) 1–9.
- [20] E. Repo, J.K. Warchol, A. Bhatnagar, A. Mudhoo, M. Sillanpää, Aminopolycarboxylic acid functionalized adsorbents for heavy metals removal from water, *Water Res.*, 47 (2013) 4812–4832.
- [21] H. Yoo, S.Y. Kwak, Surface functionalization of PTFE membranes with hyperbranched poly(amidoamine) for the removal of Cu²⁺ ions from aqueous solution, *J. Membr. Sci.*, 448 (2013) 125–134.
- [22] C. Bazzicalupi, A. Bianchi, C. Giorgi, P. Gratteri, P. Mariani, B. Valtancoli, Metal ion binding by a G-2 poly(ethylene imine) dendrimer: ion-directed self-assembling of hierarchical mono- and two-dimensional nanostructured materials, *Inorg. Chem.*, 52 (2013) 2125–2137.
- [23] V. Hoseinpour, A. Ghaee, V. Vatanpour, N. Ghaemi, Surface modification of PES membrane via aminolysis and immobilization of carboxymethylcellulose and sulphated carboxymethylcellulose for hemodialysis, *Carbohydr. Polym.*, 188 (2018) 37–47.
- [24] S.K. Ryi, N. Xu, A. Li, C.J. Lim, J.R. Grace, Electroless Pd membrane deposition on alumina modified porous Hastelloy substrate with EDTA-free bath, *Int. J. Hydrogen Energy*, 35 (2010) 2328–2335.
- [25] J.Y. Lin, W.Y. Ye, K. Zhong, J.G. Shen, N. Jullok, A. Sotto, B.V. Bruggen, Enhancement of polyethersulfone (PES) membrane doped by monodisperse stöber silica for water treatment, *Chem. Eng. Process.*, 107 (2016) 194–205.
- [26] M. Hofman, R. Pietrzak, Copper ions removal from liquid phase by polyethersulfone(PES) membranes functionalized by introduction of carbonaceous materials, *Chem. Eng. J.*, 215 (2013) 216–221.
- [27] L.Z. Song, J.B. Huo, X.L. Wang, F.F. Yang, J. He, C.Y. Li, Phosphate adsorption by a Cu(II)-loaded polyethersulfone-type metal affinity membrane with the presence of coexistent ions, *Chem. Eng. J.*, 284 (2016) 182–193.
- [28] J.J. Yong, E.Y. Choi, S.W. Kim, C.K. Kim, Fabrication and characterization of a novel polyethersulfone/aminated polyethersulfone ultrafiltration membrane assembled with zinc oxide nanoparticles, *Polymer*, 87 (2016) 290–299.
- [29] X.D. Zhao, L.Z. Song, Z.H. Zhang, R. Wang, J. Fu, Adsorption investigation of MA-DTPA chelating resin for Ni(II) and Cu(II) using experimental and DFT methods, *J. Mol. Struct.*, 986 (2011) 68–74.
- [30] X.L. Wang, L.Z. Song, C.L. Tian, J. He, S.J. Wang, J.B. Wang, C.Y. Li, DFT investigation of the effects of coexisting cations and complexing reagents on Ni(II) adsorption by a polyvinylidene fluoride-type chelating membrane bearing poly(aminophosphonic acid) groups, *Metals*, 7 (2017) 61.
- [31] S. Kasemset, L. Wang, Z.W. He, D.J. Miller, A. Kirschner, B.D. Freeman, M.M. Sharma, Influence of polydopamine deposition conditions on hydraulic permeability, sieving coefficients, pore size and pore size distribution for a polysulfone ultrafiltration membrane, *J. Membr. Sci.*, 522 (2017) 100–115.
- [32] K. Guan, W. Qin, Y. Liu, X.Q. Yin, C. Peng, M. Lv, Q. Sun, J.Q. Wu, Evolution of porosity, pore size and permeate flux of ceramic membranes during sintering process, *J. Membr. Sci.*, 520 (2016) 166–175.
- [33] L.Z. Song, R.F. Zhao, D.D. Yun, P.P. Lu, J. He, X.L. Wang, Influence of Co(II), Ni(II), tartrate, and ethylenediaminetetraacetic acid on Cu(II) adsorption onto a polyvinylidene fluoride-based chelating membrane, *Toxicol. Environ. Chem.*, 96 (2014) 362–378.
- [34] M. Hadi, M.R. Samarghandi, G. McKay, Simplified fixed bed design models for the adsorption of acid dyes on novel pine cone derived activated carbon, *Water Air Soil Pollut.*, 218 (2011) 197–212.
- [35] S.S. Madaeni, E. Salehi, Adsorption-transport modeling of anions through PVD membrane in the presence of the screen phenomenon, *Appl. Surf. Sci.*, 255 (2009) 3523–3529.
- [36] S.S. Madaeni, E. Salehi, A new adsorption-transport and porosity combined model for passage of cations through nanofiltration membrane, *J. Membr. Sci.*, 333 (2009) 100–109.
- [37] W. Shi, F. Zhang, G. Zhang, Mathematical analysis of affinity membrane chromatography, *J. Chromatogr. A*, 1081 (2005) 156–162.
- [38] J. Labanda, J. Sabaté, J. Llorens, Experimental and modeling study of the adsorption of single and binary dye solutions with an ion-exchange membrane adsorber, *Chem. Eng. J.*, 166 (2011) 536–543.
- [39] J. Labanda, J. Sabaté, J. Llorens, Modeling of the dynamic adsorption of an anionic dye through ion-exchange membrane adsorber, *J. Membr. Sci.*, 340 (2009) 234–240.
- [40] X.N. Yang, Y.P. Li, Carl T. Lira, Kinetics modeling of adsorption and desorption of benzaldehyde and benzyl alcohol on polymeric resin in supercritical CO₂, *J. CO₂ UTIL.*, 21 (2017) 253–260.
- [41] X.L. Wang, L.Z. Song, F.F. Yang, D.D. Yun, J.B. Wang, H.Y. Lu, Adsorption of Ni(II) by a polyvinylidene fluoride-type chelating membrane bearing poly(aminophosphonic acid) groups, *Desal. Wat. Treat.*, 71 (2017) 343–358.

- [42] S. Choudhari, O. Habimana, J. Hannon, A. Allen, E. Cummins, E. Casey, Dynamics of silver elution from functionalised antimicrobial nanofiltration membranes, *Biofouling*, 33 (2017) 520–529.
- [43] Y.L. Zhao, Z.G. Zhang, L. Dai, S.B. Zhang, Preparation of high water flux and antifouling RO membranes using a novel diacyl chloride monomer with a phosphonate group, *J. Membr. Sci.*, 536 (2017) 98–107.
- [44] R.K. Mishra, K. Ramasamy, S.M. Lim, M.F. Ismail, A.B. Majeed, Antimicrobial and in vitro wound healing properties of novel clay based bionanocomposite films, *J. Mater. Sci.-Mater. Med.*, 25 (2014) 1925–1939.
- [45] J.X. Leong, W.R.W. Daud, M. Ghasemi, A. Ahmad, M. Ismail, K.B. Liew, Composite membrane containing graphene oxide in sulfonated polyether ether ketone in microbial fuel cell applications, *Int. J. Hydrogen Energy*, 40 (2015) 11604–11614.
- [46] P. Yin, Y. Tian, Z.D. Wang, R.J. Qu, X.G. Liu, Q. Xu, Q.H. Tang, Synthesis of functionalized silica gel with poly(diethylenetriamine bis(methylene phosphonic acid)) and its adsorption properties of transition metal ions, *Mater. Chem. Phys.*, 129 (2011) 168–175.
- [47] Y.G. Jin, S.Z. Qiao, J.C.D. Costa, B.J. Wood, B.P. Ladewig, G.Q. Lu, Hydrolytically stable phosphorylated hybrid silicas for proton conduction, *Adv. Funct. Mater.*, 17 (2010) 3304–3311.
- [48] L. Chu, C.B. Liu, G.Y. Zhou, R. Xu, Y.H. Tang, Z.B. Zeng, S.L. Luo, A double network gel as low cost and easy recycle adsorbent: highly efficient removal of Cd(II) and Pb(II) pollutants from wastewater, *J. Hazard. Mater.*, 300 (2015) 153–160.
- [49] R. Zhao, X. Li, B.L. Sun, M.Q. Shen, X.C. Tan, Y. Ding, Z.Q. Jiang, C. Wang, Preparation of phosphorylated polyacrylonitrile-based nanofiber mat and its application for heavy metal ion removal, *Chem. Eng. J.*, 268 (2015) 290–299.
- [50] X. Li, C.C. Zhang, R. Zhao, X.F. Lu, X.R. Xu, X.T. Jia, C. Wang, L.J. Li, Efficient adsorption of gold ions from aqueous systems with thioamide-group chelating nanofiber membranes, *Chem. Eng. J.*, 229 (2013) 420–428.
- [51] W. Liu, J.S. Zhang, Y.J. Jin, X. Zhao, Z.Q. Cai, Adsorption of Pb(II), Cd(II) and Zn(II) by extracellular polymeric substances extracted from aerobic granular sludge: efficiency of protein, *J. Environ. Chem. Eng.*, 3 (2015) 1223–1232.
- [52] E. Asuquo, A. Martin, P. Nzerem, F. Siperstein, X.L. Fan, Adsorption of Cd(II) and Pb(II) ions from aqueous solutions using mesoporous activated carbon adsorbent: equilibrium, kinetics and characterisation studies, *J. Environ. Chem. Eng.*, 5 (2017) 679–698.
- [53] N.S. Ammar, A.I.M. Ismail, O.I. El-Shafey, Engineering behavior influence of basaltic rocks on the adsorption of heavy metal ions, *Desal. Wat. Treat.*, 57 (2016) 5089–5099.
- [54] Y. Liu, H. Xu, Equilibrium, thermodynamics and mechanisms of Ni²⁺ biosorption by aerobic granules, *Biochem. Eng. J.*, 35 (2007) 174–182.
- [55] H.H. Du, W.L. Chen, P. Cai, X.M. Rong, X.H. Feng, Q.Y. Huang, Competitive adsorption of Pb and Cd on bacteria-montmorillonite composite, *Environ. Pollut.*, 218 (2016) 168–175.
- [56] G.Z. Kyzas, P.I. Siafaka, D.A. Lambropoulou, N.K. Lazaridis, D.N. Bikiaris, Poly(itaconic acid)-grafted chitosan adsorbents with different cross-linking for Pb(II) and Cd(II) uptake, *Langmuir*, 30 (2014) 120–131.
- [57] J. Yang, J.X. Wu, Q.F. Lü, T.T. Lin, Facile preparation of lignosulfonate-graphene oxide-polyaniline ternary nanocomposite as an effective adsorbent for Pb(II) ions, *ACS Sustain. Chem. Eng.*, 2 (2014) 1203–1211.
- [58] G.N. Chen, K.J. Shah, L. Shi, P. Chiang, Removal of Cd(II) and Pb(II) ions from aqueous solutions by synthetic mineral adsorbent: performance and mechanisms, *Appl. Surf. Sci.*, 409 (2017) 296–305.
- [59] D.G. Liu, Z.H. Li, Y. Zhu, Z.X. Li, R. Kumar, Recycled chitosan nanofibril as an effective Cu(II), Pb(II) and Cd(II) ionic chelating agent: adsorption and desorption performance, *Carbohydr. Polym.*, 111 (2014) 469–476.
- [60] H.T. Fan, X.T. Sun, Z.G. Zhang, W.X. Li, Selective removal of Lead(II) from aqueous solution by an ion-imprinted silica sorbent functionalized with chelating N-donor atoms, *J. Chem. Eng. Data*, 59 (2014) 2106–2114.
- [61] C.P. Wang, J.Z. Wu, H.W. Sun, T. Wang, H.B. Liu, Y. Chan, Adsorption of Pb(II) ion from aqueous solutions by tourmaline as a novel adsorbent, *Ind. Eng. Chem. Res.*, 50 (2011) 8515–8523.
- [62] D.C. Yang, L.L. Yu, H. Chen, Y.B. Yu, Y.Y. Xu, J.M. Sun, Y.T. Wang, Use of apple seeds as new source for synthesis of polyacrylonitrile-based adsorbent to remove Pb(II), *Polym. Bull.*, 74 (2017) 5231–5247.
- [63] F.S. Jiryaei, A. Shahbazi, Melamine-based dendrimer amine-modified magnetic nanoparticles as an efficient Pb(II) adsorbent for wastewater treatment: adsorption optimization by response surface methodology, *Chemosphere*, 189 (2017) 291–300.
- [64] M.M. Rao, D.K. Ramana, K. Seshaiiah, M.C. Wang, S.W.C. Chien, Removal of some metal ions by activated carbon prepared from phaseolus aureus hulls, *J. Hazard. Mater.*, 166 (2009) 1006–1013.
- [65] L.Y. Hao, H.J. Song, L.C. Zhang, X.Y. Wan, Y.R. Tang, Y. Lv, SiO₂/graphene composite for highly selective adsorption of Pb(II) ion, *J. Colloid Interface Sci.*, 369 (2012) 381–387.
- [66] M. Ghasemi, A.R. Keshtkar, R. Dabbagh, S.J. Safdari, Biosorption of uranium(VI) from aqueous solutions by Ca-pretreated *Cystoseira indica* alga: breakthrough curves studies and modeling, *J. Hazard. Mater.*, 189 (2011) 141–149.